


Spring 5-8-2021

## Biomedical Porcine Models for the Study of Surgical Hemostasis, Hindlimb Ischemia, and Pancreatic Cancer

Shruthishree Aravind  
*University of Nebraska Medical Center*

Tell us how you used this information in this [short survey](#).

Follow this and additional works at: <https://digitalcommons.unmc.edu/etd>

 Part of the [Animal Experimentation and Research Commons](#), [Cancer Biology Commons](#), [Disease Modeling Commons](#), [Integrative Biology Commons](#), [Laboratory and Basic Science Research Commons](#), [Other Medicine and Health Sciences Commons](#), [Surgery Commons](#), and the [Surgical Procedures, Operative Commons](#)

---

### Recommended Citation

Aravind, Shruthishree, "Biomedical Porcine Models for the Study of Surgical Hemostasis, Hindlimb Ischemia, and Pancreatic Cancer" (2021). *Theses & Dissertations*. 522.  
<https://digitalcommons.unmc.edu/etd/522>

This Dissertation is brought to you for free and open access by the Graduate Studies at DigitalCommons@UNMC. It has been accepted for inclusion in Theses & Dissertations by an authorized administrator of DigitalCommons@UNMC. For more information, please contact [digitalcommons@unmc.edu](mailto:digitalcommons@unmc.edu).

# **Biomedical Porcine Models for the Study of Surgical Hemostasis, Hindlimb Ischemia, and Pancreatic Cancer**

by

**Shruthishree Aravind, M.D.**

A DISSERTATION

Presented to the Faculty of  
the University of Nebraska Graduate College  
in Partial Fulfillment of the Requirements  
for the Degree of Doctor of Philosophy

Medical Science Inter-Departmental Area

Under the Supervision of:

Mark A. Carlson, MD  
University of Nebraska Medical Center  
Omaha, NE

March 2021

Supervisory Committee Members:

Iraklis I. Pipinos, M.D., William H. Velander, Ph.D.,  
Vimla Band, Ph.D., and Jingwei Xie, Ph.D.

Dedicated to my grandparents Mrs. Saroja and Dr. S. Nagaraju who have taught me everything I know sincerity, hard work, dedication, honesty and compassion.

## Acknowledgements

I would like to thank all the people that have contributed to the thesis work presented here.

To my Ph.D. advisor Dr. Mark A. Carlson for his guidance.

To my supervisory committee members, Dr. Iraklis Pipinos, Dr. William Velander, Dr. Vimala Band and Dr. Jingwei Xie for their valuable time and input.

To our laboratory technicians Mr. Chris Hansen and Ms. Gerri Sifford.

To the collaborators and administrative staff in the Department of Surgery.

Most importantly, to my family, for their constant guidance, support, and love.

## Abstract

### **Biomedical Porcine Models for the Study of Surgical Hemostasis, Hindlimb Ischemia, and Pancreatic Cancer**

Shruthishree Aravind, M.D., Ph.D.

University of Nebraska Medical Center, 2021

Supervisor: Mark A. Carlson, M.D.

Murine models have dominated the world of biomedical research and comparative medicine since their development in the early 1900s. [1] While they may be suitable models to study proteomics and genomics, they may not serve as effective translational models. [2-4] Murine models do not accurately model the pathophysiology of human disease and are limited by their size, application of medical imaging and intervention, which reduces their overall preclinical predictive value. [2-4]

Porcine models on the other hand, are slowly and steadily bridging the gap between murine models and human patients. [5] Pigs are more similar to humans than rodents in terms of size, anatomy, physiology, longevity and genetics. [5-7] In the world of translational research, swine models have been replacing commonly used mammalian and primate models (for instance dogs, monkeys) for preclinical toxicologic testing of medicinal drugs. [5, 8-10] Additionally, swine models can be used as unique tools to study medical imaging (Xray, CT, MRI etc.) to better characterize and understand pathology and interventional efficacy. [11]

Our lab has been interested in producing new protocols and procedures to develop biomedical porcine models that can recapitulate human disease. In this dissertation we will present three porcine surgical models that have been developed to study human conditions with the ultimate intention to have a platform for the testing of new treatment strategies.

- 1) **Surgical Hemostasis.** In a non-survival, non-compressible hepatic resection swine model, our objective was to evaluate the acute efficacy of a hemostatic patch consisting of custom-made nano-engineered resorbable polycaprolactone (PCL) mesh embedded with human clotting factors. Normovolemic normothermic domestic swine were anesthetized, splenectomized, given a grade V liver injury and then randomized into different treatment groups of 1-hour duration. In this model of porcine hepatic resection, previously studied and standardized in our laboratory, we show that the resorbable PCL mesh, either alone or in combination with biologics, appeared to have equivalent hemostatic efficacy as the traditional surgical technique.
- 2) **Hindlimb Ischemia.** In a porcine model of hindlimb ischemia, our aim was to develop an animal model of end-organ disease for peripheral arterial disease, in order to have a platform to develop and optimize regenerative therapies. Here the domestic swine underwent open induction of right hind-limb ischemia via ligation of different arteries involved in the iliofemoral complex. FDA approved medical grade real-time X-ray fluoroscopy was used to shoot peripheral angiographies pre- and post-ligation on day zero, and then immediately prior to euthanasia on day 30, followed by necropsy. Cross comparison of the different ligation models produced measurable difference in end points - arterial pressure, muscle oxygen saturation, and treadmill stamina. We provide histological evidence of myopathy in the porcine model were comparable with human counterparts.
- 3) **Pancreatic Cancer.** In a novel porcine model of pancreatic cancer, our intention was to induce pancreatic ductal adenocarcinoma in a large animal (transgenic KRAS/p53 Oncopig) whose size was comparable with humans, which would provide us with a platform to use and test diagnostic and therapeutic strategies.

AdCre injection of the transformed cells into the pancreatic duct and the parenchyma of five Oncopigs after four months failed to produce gross tumors but did show histological evidence cell proliferation with transgene expression.

In conclusion, we show that these porcine surgical models are potential translational animal models that can mimic human disease and may provide more relevant data compared to rodent models. In these large animal models, we were able to use clinically relevant techniques, such as advanced medical imaging, to characterize and quantify the disease process which would not have been possible in murine models. Additionally, we demonstrated that these models could provide unique opportunities to test and develop novel diagnostic methods and therapies.

# Table of Contents

<b>Acknowledgements.....</b>	<b>iii</b>
<b>Abstract.....</b>	<b>iv</b>
<b>Table of Contents .....</b>	<b>vii</b>
<b>List of Figures.....</b>	<b>x</b>
<b>List of Tables.....</b>	<b>xi</b>
<b>List of Abbreviations.....</b>	<b>xii</b>
<b>CHAPTER 1: Background and Significance .....</b>	<b>2</b>
<b>1.1 Animal Models.....</b>	<b>2</b>
<b>1.2 Porcine Models.....</b>	<b>3</b>
<b>CHAPTER 2.....</b>	<b>7</b>
<b>Porcine Model of Hepatic Resection for the evaluation of Biologics- Supplemented Hemostatic Patch.....</b>	<b>7</b>
<b>2.1 Introduction .....</b>	<b>7</b>
<b>2.2 Materials and Methods .....</b>	<b>3</b>
<b>2.3 Results.....</b>	<b>16</b>



<b>2.4 Discussion .....</b>	<b>21</b>
 <b>CHAPTER 3 .....</b>	 <b>24</b>
<b><i>Porcine Model of Hindlimb Ischemia.....</i></b>	<b><i>24</i></b>
<b>3.1 Introduction .....</b>	<b>24</b>
<b>3.2 Materials and Methods .....</b>	<b>27</b>
<b>3.3 Results.....</b>	<b>41</b>
<b>3.4 Discussion .....</b>	<b>43</b>
 <b>CHAPTER 4 .....</b>	 <b>46</b>
<b><i>Porcine Model of Pancreatic Cancer .....</i></b>	<b><i>46</i></b>
<b>4.1 Introduction .....</b>	<b>46</b>
<b>4.2 Materials and Methods .....</b>	<b>49</b>
<b>4.3 Results.....</b>	<b>57</b>
<b>4.4 Discussion .....</b>	<b>61</b>
 <b>CHAPTER 5 .....</b>	 <b>63</b>
<b><i>Overall conclusions .....</i></b>	<b><i>63</i></b>
 <b>CHAPTER 6 .....</b>	 <b>65</b>

<i>Future Directions</i> .....	65
--------------------------------	----

<i>REFERENCES</i> .....	67
-------------------------	----

## List of Figures

<b>Figure 1.</b> Hemorrhage Model - Workflow.....	6
<b>Figure 2.</b> Hemorrhage Model - PCL bandage .....	7
<b>Figure 3.</b> Hemorrhage Model - PCL bandage application.....	12
<b>Figure 4.</b> Hemorrhage Model - PCL bandage post-application .....	13
<b>Figure 5.</b> Hemorrhage Model - Necropsy Specimen.....	15
<b>Figure 6.</b> Ischemia Model - Workflow .....	28
<b>Figure 7.</b> Ischemia Model - Operative Setup.....	31
<b>Figure 8.</b> Ischemia Model – End Points.....	32
<b>Figure 9.</b> Ischemia Model - Ameroid Model.....	35
<b>Figure 10.</b> Ischemia Model - Ligation Model .....	37
<b>Figure 11.</b> Ischemia Model - H&E images of myopathy .....	42
<b>Figure 12.</b> Pancreatic Cancer Model - Workflow.....	50
<b>Figure 13.</b> Pancreatic Cancer Model - Injection sites.....	53
<b>Figure 14.</b> Pancreatic Cancer Model - Necropsy specimen.....	55
<b>Figure 15.</b> Pancreatic Cancer Model - H&E images of pancreas .....	57
<b>Figure 16.</b> Pancreatic Cancer Model - H&E images of pancreas .....	58
<b>Figure 17.</b> Pancreatic Cancer Model - IHC images of pancreas .....	59

## List of Tables

<b>Table 1.</b> Coagulation factors – Physiological level .....	11
<b>Table 2.</b> Hemorrhage Model – Baseline animal characteristics .....	17
<b>Table 3.</b> Hemorrhage Model – 10 min post injury.....	18
<b>Table 4.</b> Hemorrhage Model – 60 min post injury.....	19
<b>Table 5.</b> Ischemia Model – End point measurements .....	41

## List of Abbreviations

1. AAALAC      Association for Assessment and Accreditation of Laboratory  
Animal Care International
2. ABG          Arterial Blood Gas
3. ABI          Ankle/Brachial Index
4. ANOVA      Analysis of Variance
5. ARF          Animal Research Facility
6. CBC          Complete Blood Count
7. CG          Combat Gauze™
8. CLI          Chronic Limb Ischemia
9. CIIT          Common Internal Iliac Trunk
10. DFSD      Dry Fibrin Sealant Dressing
11. DOD          Department of Defense
12. FI          Factor I (fibrinogen)
13. FII          Factor II (thrombin)
14. FXIII      Factor XIII (crosslinking factor)
15. FDA          Food and Drug Administration

16. FS	Fibrin Sealant
17. H&E	Hematoxylin and Eosin
18. IACUC	Institutional Animal Care and Use Committee
19. IHC	Immuno Histo Chemistry
20. LEIA	Left External Iliac Artery
21. LIIA	Left Internal Iliac Artery
22. LPFA	Left Profunda Femoral Artery
23. MAP	Mean Arterial Pressure
24. PCL	Polycaprolactone
25. pd-FS	plasma-derived fibrin sealant
26. pd-FXIII	plasma-derived Factor XIII
27. rFI	recombinant Factor I (fibrinogen)
28. rFII	recombinant Factor II (thrombin)
29. rFXIIIa	activated recombinant human Factor XIII
30. rFS	recombinant fibrin sealant
31. REIA	Right External Iliac Artery
32. RLCIA	Right Lateral Circumflex Iliac
33. RLCFA	Right Lateral Circumflex Femoral Artery
34. RIIA	Right Internal Iliac Artery

35. RPFA	Right Profunda Femoral Artery
36. RSFA	Right Superficial Femoral Artery
37. RPop	Right Popliteal Artery
38. PAD	Peripheral Arterial Disease
39. Moxy	Muscle Oximetry
40. StO <sub>2</sub>	Muscle oxygen saturation
41. THb	Total Hemoglobin
42. UNL	University of Nebraska—Lincoln
43. UNMC	University of Nebraska Medical Center

# CHAPTER 1: Background and Significance

## *1.1 Animal Models*

An ideal animal model of human disease should possess certain characteristics:

1. The animal model should closely resemble the pathophysiology of human disease and should be relatively easy to induce it in the host. [8]
2. The animal model should possess a similar route of disease induction and progression. [8]
3. The model should be inexpensive, easy to manipulate and maintain. [8]
4. These models should have a fairly short course of the target disease. [8]
5. Despite the interspecies variability between humans and animals, the animal model should produce a measurable, comparable disease equivalence. [8]

Mice have remained the powerhouse of biomedical research for more than six decades. [1] More than 95% of the animal models used in biomedical research in North America are based on the mice. [1, 12] 61% of laboratory animals used in Europe are mice. [13] Mice dominantly represent the biomedical research all over the world, as they are readily available to purchase in large quantities, a relatively small size makes them easier to house, maintain and handle, which makes them very inexpensive. [1]

Furthermore, mice breed rapidly (once every 3 months) producing a large litter in about 20 days. [1, 14] Additionally, researchers are provided with a wide variety genetically stable inbred strains or heterozygous outbred strains, which makes them useful animal models in a wide spectrum of experiments. [1, 14] Advancement in genetic engineering have increased the ability of commercial laboratories to easily modify the animal strain in order to tailor the needs of a researchers experiment. [1, 14]



Despite remarkable technological advancement and complete control of researchers over mouse models, especially in the last few decades progress in medical science has been much slower. [15] While these are excellent tools to study molecular biology, they do not always mirror the heterogeneity and complex characteristics of human diseases and cancer. [2-4] As translational models, murine models show less-than-optimal predictability as evidenced by the low FDA approval rate (<5%) for candidate anti-cancer therapies (i.e., drugs coming out of preclinical drug testing). [2-4] On an average, only 5 out 5000 drug discoveries proceed from pre-clinical testing to phase 1 clinical trials. [2-4] Out of the 5 drugs approved for randomized control trials only one is approved by FDA. [2-4] Drugs that have shown efficacy in mouse models have failed to produce any effect in human subjects questioning the validity and predictability of mouse models in translational research.[2-4] Developmentally mice and humans are approximately 80 million years apart, sharing nearly 90% of the genome sequence in the protein coding regions, but are less conserved or dissimilar in the non-coding and regulatory regions. [16] Several researchers have described the inherent difference in the molecular, genetic and immunologic makeup between humans and mice that makes the cancer development different between the two species. [4, 9, 17] Furthermore, due to the small size of the murine models, there is limited feasibility to study interventional systems (e.g., intensity-modulated radiation therapy). [15, 18]

## *1.2 Porcine Models*

With the first draft of the porcine genome in 2012, the pig has been emerging as an important translational model for many human diseases. [5, 19] The porcine-human genetic homology in coding regions appears to be greater than that of murine-human genetic homology, and the porcine DNA methylation pattern is highly conserved with

respect to humans. [6, 20] There also is anatomic, physiologic, immunologic and metabolic similarity between humans and pigs, which facilitates the latter as platform to study multitude of human diseases. [5, 6, 10, 20]

There are several clear advantages that makes the pigs an ideal translational model to study complex human diseases. [7] Pigs are easily available as they are one of the most common livestock species used for human consumption. [7] Over 500 breeds of inbred and outbred pigs exist in this world. [7] The typical weight of various minipig strains ranges from 40-60 kg, which is reasonably close to human size, as opposed to a 20 g mouse. [5, 7, 9, 10] Pigs attain sexual maturity at 6 months of age, have a short gestation period of about 4 months (or 114 days), produce an average of 10–12 piglets/litter or an average of 24–36 piglets/year. [7] They have short generation interval of about 12 months and enjoy an all-season breeding. [7] The average lifespan of mice is <2 years, whereas the average lifespan of pig is 10- 20years, which also brings the pig closer to the human condition. [7, 9] Physiologically pigs are similar to humans omnivorous and have the ability to survive both on plants and animal matter. [7] While being expensive, experimental pig handling, housing, and monitoring have been standardized and the last 15 years, the porcine research world has seen rapid development in cloning and transgenic technologies. [3, 7, 10, 19] Additionally, porcine-directed research tools like cell lines, enzymes antibodies, ELISA etc. are easily available for purchase.

Pharmacokinetics, pharmacodynamics and drug distribution in the pig is similar to humans. [5, 10, 21] More than half of the prescription medications in humans are metabolized by cytochrome p450 (cytochrome p450) enzyme, the level of which is comparable in pigs. [21] On the other hand, the cytochrome p450 level in mice is twice that of humans, resulting in a differing drug metabolism. [10, 21] Hence the utilization of

pig models in preclinical drug trials can provide us with a better prediction of drug safety and efficacy prior to investing in human clinical trials. [21]

Like the primate animal models, pigs will produce a tangible resultant pathology (for instance - tumor, atherosclerosis etc.) that can be used to study imaging, radiation therapy and photodynamic therapy etc. [11] These models can be used to perform various surgical procedures and collect multiple samples. A porcine model of human disease will provide a platform to develop and study noninvasive imaging techniques and novel therapeutic drugs for clinical application. [22] The size of the porcine subjects will permit studies on both diagnostic and therapeutic technologies that would be difficult in mice. [22] In addition, the porcine models of human disease likely would be more predictive of human response to novel anti-tumor therapies than the equivalent murine model, as the pig is the better mimic of human biology providing a bridge between small animal models and human cohorts. [3-5, 8, 10, 11, 15]

When using pigs as animal models for biomedical research, one should be aware that they come with certain limitations. Pig handling depending on their size requires special equipment and trained personnel and can be more expensive when compared to the cost of handling small animals. [18] Isolation of pigs other than in individual pens can be difficult especially when research involves working with recombinant DNA technology. [18] Additionally, pigs can get reach up to sizes greater than 150 Kgs and it will be very difficult and maybe next to impossible to work with aged porcine subjects. [18] In contrast, small animals can be easily isolated using a micro-incubator and can be easily handled as aged subjects. [18] One must be cognizant about these limitations before choosing pigs as models for biomedical research.

The purpose of this article is to present the design and details of three surgical swine models, their maintenance and management in a laboratory setting, and to outline their use of in biomedical research.

## CHAPTER 2

### Porcine Model of Hepatic Resection for the evaluation of Biologics-Supplemented Hemostatic Patch

The materials presented in this chapter will be submitted to a peer-reviewed journal

#### *2.1 Introduction*

In United States, unintentional injuries are the leading cause of death in young persons in the age range of 5-45 years of age. [23-25] It disproportionately affects younger individuals particularly young males. [26] According to SEER (Surveillance, Epidemiology, and End Results) epidemiological data after Cardiovascular diseases and Cancer; Injuries is the third leading cause of death in United States. [26] Amongst the unintentional injuries, trauma-induced acute exsanguination (hemorrhage) is the second leading cause of morbidity and mortality. [23-25, 27] Multiple studies have estimated that after traumatic brain injury (42%-52%), hemorrhage (30%-39%) accounts for approximately 35% of pre-hospital deaths and nearly 40% of these deaths occur within the first 24 hours of injury making it the leading cause of preventable deaths under the age of 45. [24, 25, 27]

Very recently in 2020, the World Health Organization (WHO), reported that each year motor vehicle crashes claims 1.35 million lives and mostly affects people from the

low- and middle-income developing countries. [28] In United States alone, approximately 2.3 million people are admitted to the emergency department each year from motor vehicle related injuries. [29] Each year, motor vehicle crashes claims nearly 35,000 lives in United States. [27] As a result they cost the government 10% of the total healthcare expenditure which is about \$44 billion dollars each year on medical expenses. [28]

The WHO has most recently described the trauma related injuries as “Neglected Epidemic”. [30] While deaths due to traumatic brain injuries are largely not preventable, deaths secondary to hemorrhage are potentially preventable. [24, 25, 27] Improving outcomes in this group starts in the field, the moment the patient is injured with hemorrhage control combined with resuscitation and rapid transport by the EMS to a treatment center. [25]

There are two major categories of bleeding, compressible and non-compressible. [31] Compressible hemorrhage is extremity hemorrhage where the bleeding can be controlled using direct digital pressure, tourniquet or a pressure dressing. [31] Non-compressible hemorrhage is a truncal (thoraco-abdomino-pelvic) or junctional (perineum, groin, axillary) hemorrhage. [31] In the majority of the times, non-compressible hemorrhage is intracavitary involving a solid organ and is simply not amenable to compression. [31] Early resuscitation and faster transport to the treatment center are the only treatment options available for the truncal non-compressible hemorrhage. [25, 27, 31] The Committee on Tactical Combat Casualty Care (CoTCCC) in collaboration with several organizations is making a substantial effort in developing an effective treatment and improving outcomes in non-compressible hemorrhage patients. [32, 33]

### Food and Drug Administration (FDA) approved Hemostatic Dressings

The US military has recently approved a chitosan-based dressing and a granular zeolite mineral powder containing dressing for the field treatment of non-compressible hemorrhage. [31, 33] These worked by adhering to the bleeding tissues, concentrating the clotting factors and sealing the blood vessels but their efficacy diminished with time. [31-33] The chitosan-based dressings alone or with the addition of smectite minerals were derived from chitin, a protein derived from shrimp tail which is allergy prone and led to the formation of intravascular thrombo-emboli. [32-34] The QuickClot granules containing the zeolite powder produced rapidly absorbed water in the tissues and produced exothermic reaction, which has resulted in second and third degree burn at the site of application. [32-34] Then a Dry Fibrin Sealant Dressing (DFSD) was developed from virus inactivated fibrinogen and thrombin of human plasma. [31, 32] The biggest disadvantage of DFSD, that limited its widespread use were its cost and storage requirements. [32-34] Lastly, a surgical gauze impregnated with kaolin and aluminum silicate called the QuikClot® Combat Gauze™ was approved by the Committee on Tactical Combat Casualty Care (CoTCCC). [31, 32] It activated the intrinsic pathway of the clotting system without any side effects and so the QuikClot® Combat Gauze™ was termed as “the hemostatic dressing of choice” for compressible hemorrhage by the Committee on Tactical Combat Casualty Care (CoTCCC). [31-33] These are non-absorbable, non-biologic meshes which may be ineffective in hypo-coagulopathic individuals. [32]

To overcome these disadvantages, we utilized an extremely cost-effective recombinant fibrinogen isolated by our collaborators, which when applied through the nano-engineered polycaprolactone (PCL) bandage material, will only need 20-fold less

fibrin sealant than that is used by the Dry Fibrin Sealant Dressing (DFSD). [35] The cost of our fibrin sealant dressing is projected to be <\$100 per unit. [35]

### Coagulation Cascade

Coagulation cascade is a series of dynamic and interwoven protein-protein interaction that takes place when there is endothelial injury which leads to the formation of firm fibrin clot which seals the blood vessel and prevents blood loss. [36] An insult or injury to a blood vessel exposes the subendothelial collagen to blood, which activates two sets of pathways, intrinsic and extrinsic pathway. [36] Activation of the intrinsic pathway and the extrinsic pathway leads to a series of clotting factor activation converging into a common pathway. [36] In common pathway, active factor IX (from extrinsic pathway) and active factor VII (from intrinsic pathway) both activate factor X to activated Xa which in the presence of factor V and calcium convert prothrombin (factor II) to thrombin (active factor IIa). [36] Thrombin is a procoagulant enzyme which converts fibrinogen (factor I) to fibrin monomer (active factor Ia). [35, 36] Activated factor XIIIa (fibrin stabilizing factor) crosslinks fibrin monomers into long stable fibrin polymer forming a stable clot consisting of RBCs and platelets which seals of blood vessels. [35, 36] Thus, fibrinogen acts as a principal structural component of the clotting mechanism in the body. [35, 36] Advancement in recombinant DNA technology has led to the development of numerous clotting products that have been used exogenously to enhance the hemostasis. [37]



Table 1. Physiologic levels of Coagulation Factors and their half-life.

<b>Coagulation Factor [38, 39]</b>	<b>Half Life (hours) [39]</b>	<b>Plasma Concentration [38, 39]</b>
<b>I (Fibrinogen) (mg/dl)</b>	90	240 (200-400) (mg/dl)
<b>II (Prothrombin) (%)</b>	60	95 (80-120)
<b>V (%)</b>	12-36	120 (50-150)
<b>VII (%)</b>	6	100 (65-140)
<b>VIII (%)</b>	12	90 (65-115)
<b>IX (%)</b>	24	110 (60-140)
<b>X (%)</b>	40	105 (45-155)
<b>XI (%)</b>	60	100 (65-135)
<b>XII (%)</b>	48-52	130 (50-150)
<b>XIII (%)</b>	72-120	100 (68-138)

There are two main types of commercial clotting factors that are available, “Plasma-derived” Factor Concentrates, and “Recombinant” Factor Concentrates. [37, 40] “Plasma-derived” Factor Concentrates are isolated from pooled plasma from donated blood. [37, 40] The different clotting factors are isolated from plasma after it undergoes serial washes with several chromatographic and fractionation techniques. [40] The isolated clotting factors are freeze dried into a powder form which then undergoes further processing like heat treatment, microfiltration for virus inactivation. [40] The downside to

using “Plasma-derived” Factor Concentrates is its cost, need for reconstitution before use and storage requirements. [40]

In the early 90s the Food and Drug Administration (FDA) approved different “Recombinant” Factor Concentrates for the treatment of different hematologic diseases. [40] “Recombinant” Factor Concentrates are commercially manufactured genetically engineered factors using recombinant DNA technology. [40] Here the DNA fragment coding for the clotting factors is isolated and integrated into the host DNA of an animal cell line using a plasmid vector. [40] The recombinant protein can then be produced in large amounts by stimulation of the cDNA (chimeric DNA) in cell culture. [35, 37] Although the “Recombinant” Factor Concentrates are cheap and pathogen free, these concentrates lack human specific post-translational modification and subsequently optimal protein function. [37] Additionally, “Recombinant” Factor Concentrates tend to mount an immune response with repeated use as they are antigenically different from the endogenous proteins. [40]

With an overall goal to develop a synthetic resorbable biologics-supplemented bandage to control bleeding involving solid organs (liver, spleen, kidney), our research project seeks to address the challenging problem of truncal non-compressible hemorrhage in civilian and combat trauma. In collaboration with University of Nebraska-Lincoln, our laboratory has developed an economical source of human fibrin sealant, along with a technology to produce resorbable, nano-engineered mesh. [41] With appropriate implementation techniques, this will improve efficacy of solid organ surgery especially in terms of decreased blood loss, shortened operative time and decreased post-operative mortality. [41] Finally, the long-term objective of this research project is to extend this into survival studies in animal models with the ultimate goal of seeking FDA approval for use in clinical surgeries.

### *Specific Aim:*

Our goal was to test the acute efficacy of fibrin sealant (containing human plasma-derived fibrinogen, human recombinant thrombin and human recombinant Factor XIII) supplemented Polycaprolactone (PCL) bandages in a porcine liver surgical resection model.

### *Hypothesis:*

Polycaprolactone (PCL) mesh embedded with biologics has equivalent hemostatic efficacy compared to traditional surgical technique in a porcine liver resection model.

## *2.2 Materials and Methods*

### *Study Design*

This is a pre-clinical, non-human, exploratory study to evaluate the acute efficacy of a hemostatic patch; resorbable polycaprolactone (PCL) mesh embedded with human clotting factors. This study used a porcine experimental trauma model to do the preclinical testing.

### *Sample Selection and Inclusion/Exclusion criteria*

Since the swine models share similar anatomic, physiologic and biochemical characteristics with humans, young domestic Yorkshire random-bred pigs were used in this study. Yorkshire pigs were chosen because of their easy availability and maintenance. Also, manual handling of the animals is easy when the animals are younger and smaller. Experimental animals for the study were in the age range of 3-5 months and were purchased from the Agricultural Research and Development Center (Mead, NE).

#### Inclusion Criteria: [42]

1. Body weight: 32-42 kg
2. Hematocrit: 27%-40%
3. Platelet count: ~200 K/mm<sup>3</sup>
4. Prothrombin Time less than or equal to 14 s
5. Partial Thromboplastin Time less than or equal to 25 s
6. Fibrinogen: ~ 100 mg/dL

#### Exclusion Criteria: [42]

1. Persistent low MAP (<55 mm Hg) at the baseline
2. Persistent hypotension and unresponsive to fluid resuscitation despite no bleeding

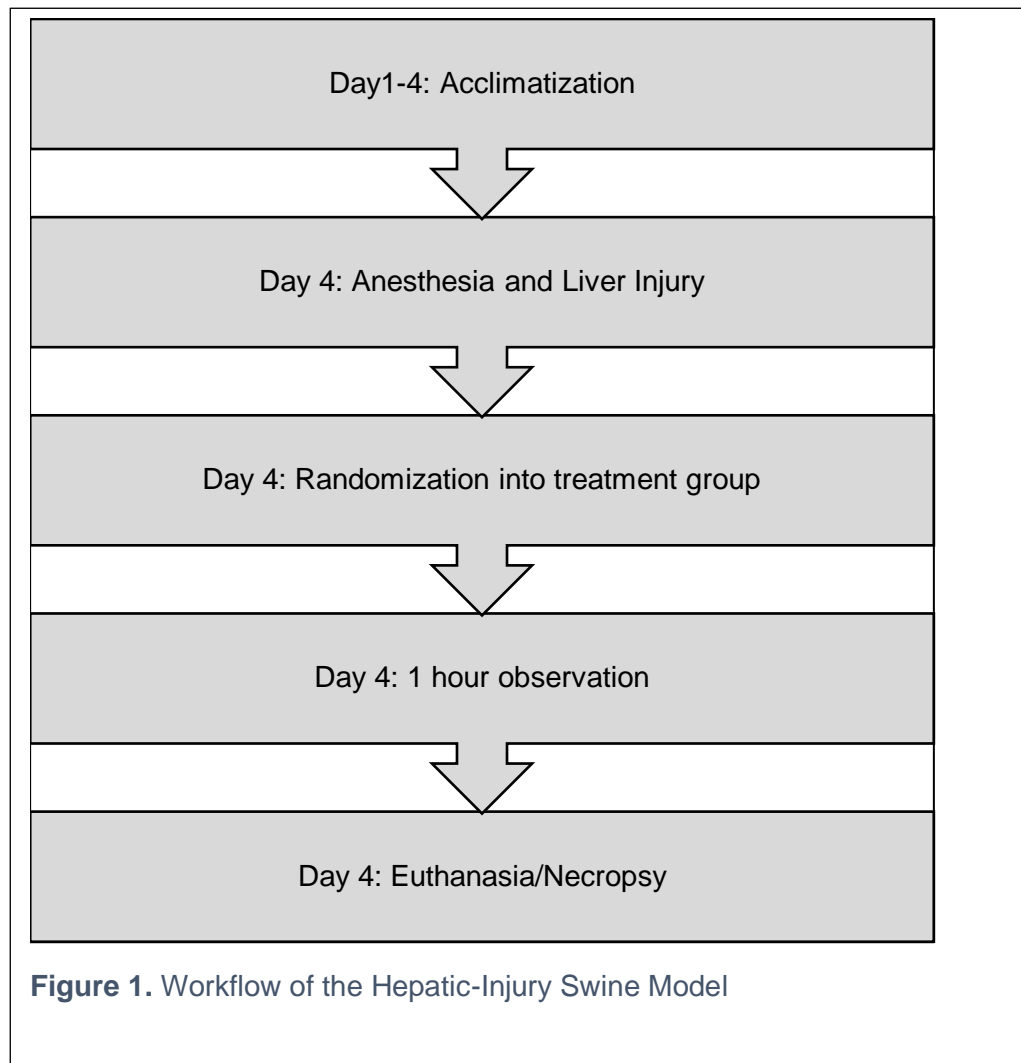
#### Animal Welfare

Recommendation from National Institutes of Health detailed in the Guide for the Care and Use of Laboratory Animals (8th ed.) was used to ethically carry out all of the experimental procedures in this study protocol. [43] The animal protocol for the study was reviewed in detail and approved by the Institutional Animal Care and Use Committee of the VA Medical Center in Omaha, Nebraska. The VA Medical Center research facility is approved by Association for Assessment and Accreditation of Laboratory Animal Care International (AAALAC) and all procedures were performed in the AAALAC approved facilities. [43]

#### Randomization of Study Groups

A minimum number of (n=12) swine were randomized into four different experimental groups and this number was drawn to maintain a statistical power (1 -  $\beta$ ) of

0.8 false positive rate ( $\alpha$ ) of 0.05, false negative rate ( $\beta$ ) of 0.2. [44] Cohen's d statistical formula  $\Delta/\sigma$  ( $\Delta$  is the difference between the means and  $\sigma$  is the standard deviation) was used to determine these numbers. [44] The intent of this study was to test the acute efficacy of test bandages in in-vivo studies utilizing the grade 5+ pig liver surgical resection models. Porcine subjects will be randomized among four treatment groups: group 1 (control) = cautery + suture ligation + Surgicel® application; group 2 = PCL mesh alone (16 x 8cm, six-ply); group 3 = PCL with fibrin sealant (FS = human plasma-derived fibrinogen (pdFI) + human recombinant thrombin (rFII) + human recombinant Factor XIII (rFXIII)); group 4 = PCL with rFII + rFXIII only. The outcomes measurements of experiment included survival at 60 min, blood loss (mL), systemic arterial blood pressure (mm Hg), body temperature, shock index (SI), arterial blood gas, and hematocrit.



### Experimental Dressing



**Figure 3. (A)** PCL Bandage prior to its experimental use (Size 16 cm x 8 cm)

Using a unique engineering approach, a re-absorbable, pliable, Poly (D, L lactide) (PLA) mesh from medical grade biopolymer using a proprietary, high-speed electro hydrodynamic (EHD) production spinneret was developed (LNK Chemsolutions; Lincoln NE). [45] The polycaprolactone (PCL) mesh is designed to be microporous enabling co-polymerization of endogenous blood clots with exogenously applied clotting factors, also known as Fibrin Sealant (FS). [45] In addition, these nano-engineered meshes hold twenty-fold less fibrin sealant/biologics than the currently marketed hemostatic dressings. [45]

### Animal Preparation

Fifty-one Yorkshire random-bred commercial swine, all castrated males, aged ~3 months weighing 33–40 kg were brought from Agricultural Research and Development Center (ARDC) at Mead, Nebraska. Animals were housed indoors in individual cages under SPF (specific-pathogen free) conditions. During the 3-4-day acclimatization period, the animals had free access to water and were fed a corn and soybean based meal. [46]

### Induction and Anesthesia

Animals were fasted for at least 12 hours before the surgical procedure. [47] During this time, they had free access to drinking water. [47] Anesthesia induction for each animal was with a single 3 mL intra-muscular premixed cocktail injection containing 150 mg Telazol (Zoetis; 4.4mg/kg), 90 mg ketamine (Zoetis; 2.2mg/kg), and 90 mg xylazine (Zoetis; 2.2 mg/kg). [46] To minimize hypersalivation intramuscular atropine sulfate at a dose of 0.05 mg/kg was used on an as needed basis. Each animal was weighed and orotracheally intubated using a 7.0mm - 7.5 mm cuffed tube. [46] A peripheral line was placed in an auricular marginal vein as an additional access to administer fluids or medication. [34, 48, 49] Electrocardiogram monitor, buccal pulse oximeter and rectal temperature probe were placed. To maintain the body temperature at 37 C, animals were rested on a water-circulated heating pad. [34, 48, 49] Anesthesia was maintained with isoflurane (1%-2%) mixed with oxygen (1L-2L). [48] Throughout the procedure animals were mechanical ventilated in a pressure control mode delivering 13-15 breaths/minute, with a tidal volume of 5-10mL/kg, and the end-tidal partial pressure of CO<sub>2</sub> at 30–45 mm Hg. [34, 48, 49]

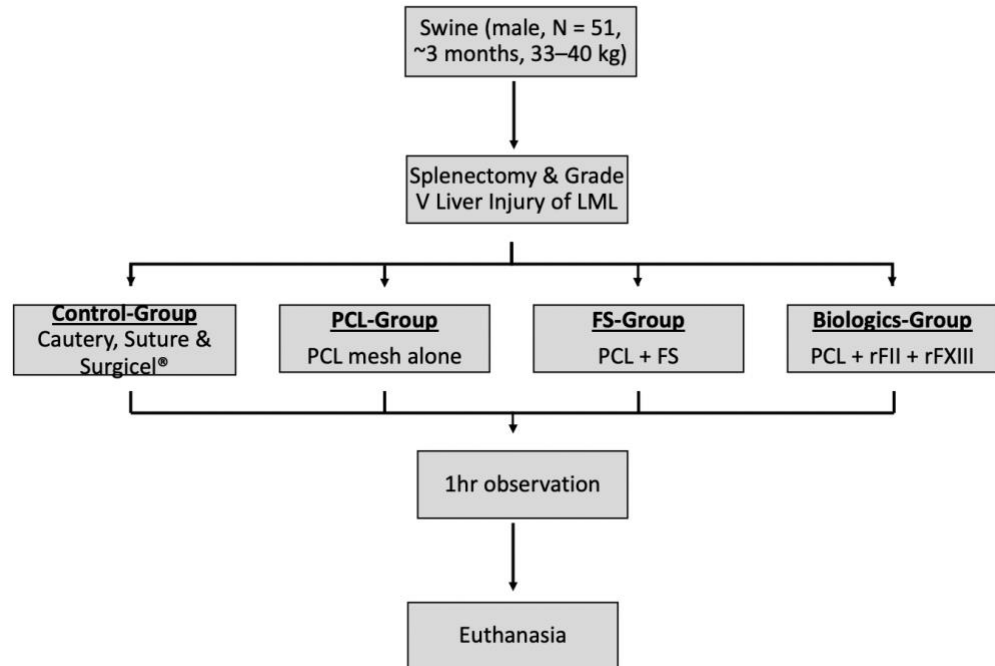
Then a 5 cm cutdown procedure was performed along the sternocleidomastoid muscle border. [47] Next, the right carotid artery (20 gauge) and the right internal jugular vein (16 gauge) were canalized for arterial pressure monitoring and isotonic fluid



administration respectively. [48] Vital signs were continuously monitored and recorded by a Bionet monitor. [48] First set of blood samples were collected through the arterial line in the internal carotid artery for a complete blood count (CBC), arterial blood gas analysis (ABG) and a complete coagulation profile consisting of prothrombin time (PT), international normalized ratio (INR) and plasma fibrinogen level were performed. Then a ventral midline laparotomy incision was performed extending from the xiphoid process into the groin. [34, 48, 49] The incision was then carried to the subcutaneous tissue and musculoaponeurotic layers using a bipolar cautery. Peritoneum was carefully entered, and a splenectomy was performed after the arteries and veins entering the spleen were ligated. [34, 48, 49] A trans-abdominal urinary bladder catheterization is performed using an 18 French Foley catheter. [34, 48, 49] A volume equivalent of warm Lactated Ringers (LR) that is three times the weight of excised spleen and pre-injury blood loss was infused rapidly through the jugular line. [34, 48, 49]

#### *Injury Mechanisms*

Hepatic Left Medial Lobe Hemi-transection (LMLH): This liver-injury model was used to produce American Association of Surgical Trauma (AAST) grade V liver injury. [34, 48, 49] The left medial lobe of the liver was first identified, mobilized and exteriorized by bringing it out into the operative field. [47] The left medial lobe was then gently held between the index finger and the middle finger and using a cautery, a line of resection on the LM lobe 3 cm distal from the junction with RM lobe was marked with electrocautery (see fig 3A). [47] The left medial lobe of the liver was excised using a sharp mayo scissors. (see fig 3B)



Immediately after resection, the animals were randomized into either of the 4 treatment groups.

1. Group 1 (control) = Cautery + Suture ligation + Surgicel® application; This was a “control” resection, in that the bleeding was handled with clamping/tying, suture ligatures, and electrocautery (Surgicel® is an absorbable matrix for platelet adhesion and aggregation made of oxidized regenerated cellulose used to control capillary, venous and small arterial hemorrhage). Group 1 served as a ‘positive control’ in this experimental setup. Positive control by definition, produces an effect in the positive direction when there is an active intervention. [50] Negative control are treatment conditions that are set out to show an outcome under standardized conditions in the absence of an intervention. [50] A negative control for the aim of this study would be to perform a grade V liver injury on the porcine subjects and to observe them for 60 mins with no intervention. In real world, when treating a patient with grade V liver injury, a surgeon will intervene, try to stop the bleeding or perform

a “damage control” control. Absence of real-world true negative control scenarios prompted us to compare our experimental groups with a positive control.

2. Group 2 = PCL mesh alone (folded to a final dimension of 16 x 8cm, six-ply); was applied flat onto the resection surface. Bimanual compression was held for about 5 minutes.
3. Group 3 = PCL with fibrin sealant (FS = human plasma-derived fibrinogen (pdFI) + human recombinant thrombin (rFII) + human recombinant Factor XIII (rFXIII)); the PCL bandage sprayed with biologics was applied onto the bleeding surface with additional biologics then were sprayed onto the exposed PCL surface and bimanual compression was held for 5 minutes.
4. Group 4 = PCL with rFII + rFXIII only; the PCL bandage sprayed with biologics was applied onto the bleeding surface with additional biologics then were sprayed onto the exposed PCL surface and bimanual compression was held for 5 minutes.

At the end of 5 min compression, the excised left medial liver lobe was removed, the pooled blood was collected, blood-soaked sponges weighed, final photographs were taken, and the abdomen was temporarily closed using penetrating towel clamps.

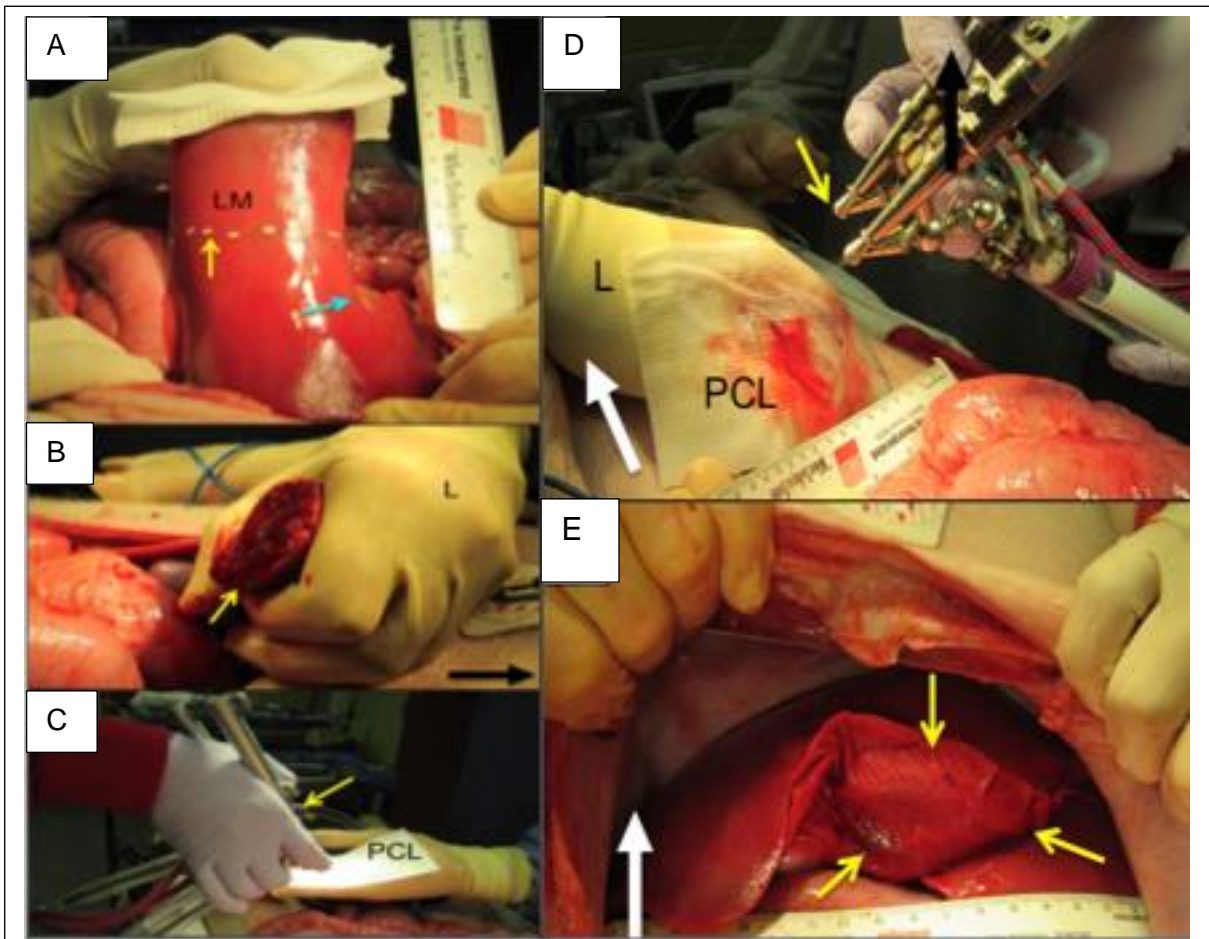


**Figure 5.** (A) LM Lobe held out and marked (yellow arrow-resection line, blue arrow-LM intersection with RM lobe). (B) Pincer grip to base of LM lobe. (C) PCL bandage sprayed with biologics. (D) PCL bandage applied to injury site; additional biologics sprayed. (E) Post treatment view of the abdomen, PCL bandage on the injury site (yellow arrows) after 5min compression.

LM Lobe-Left Medial Lobe, RM Lobe-Right Medial Lobe, PCL-Polycaprolactone

### Post-injury Management

The post-injury observation period was standardized for 1 hour. [47] The target Mean Arterial Pressure (MAP) was standardized to 80% of the pre-injury value. [47] During the observation period if the MAP dropped below the calculated target MAP, LR resuscitation at a rate of 150 mL/min was initiated. [47]

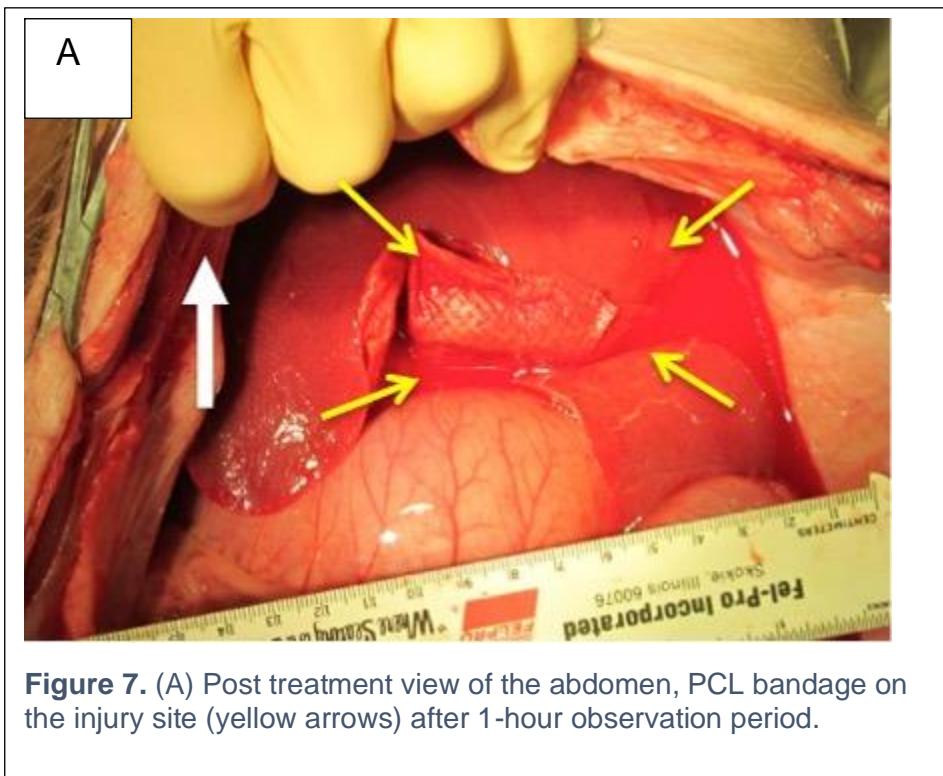


**Figure 7.** (A) Post treatment view of the abdomen, PCL bandage on the injury site (yellow arrows) after 1-hour observation period.

### Euthanasia

At the end of 60 min observation period, if the animals survived, euthanasia and necropsy of the animal was performed first by increasing isoflurane inhalation to 5%. [51] 60-minute post procedure all post-injury blood loss was collected, and the blood-soaked laparotomy sponges were weighed. [47] The diaphragm was then transversely incised attempting to expose the supradiaphragmatic inferior vena cava which is then transected. [51] Animal subjects that did not survive the 60 minute observation period, had post procedure blood loss measured followed by necropsy, in accordance with AVMA Guidelines. [51] According to AVMA guidelines, death was defined as MAP <10 mm Hg with no identifiable pressure wave tracing. [51]

### Endpoints

The primary endpoints were vital signs like the heart rate, mean arterial pressure (MAP), rectal temperature, oxygen saturation, EKG and end tidal partial pressure of CO<sub>2</sub> was continuously recorded throughout the procedure. Blood samples from carotid artery and jugular vein were collected after 15 min and 60 min post-injury to measure the secondary end points to measure the hemoglobin, hematocrit, platelet counts, pH, lactate, base deficit, and complete coagulation profile (PT, INR, fibrinogen, and TEG parameters). Finally, the liver is necropsied, inspected, dissected, and photographed.

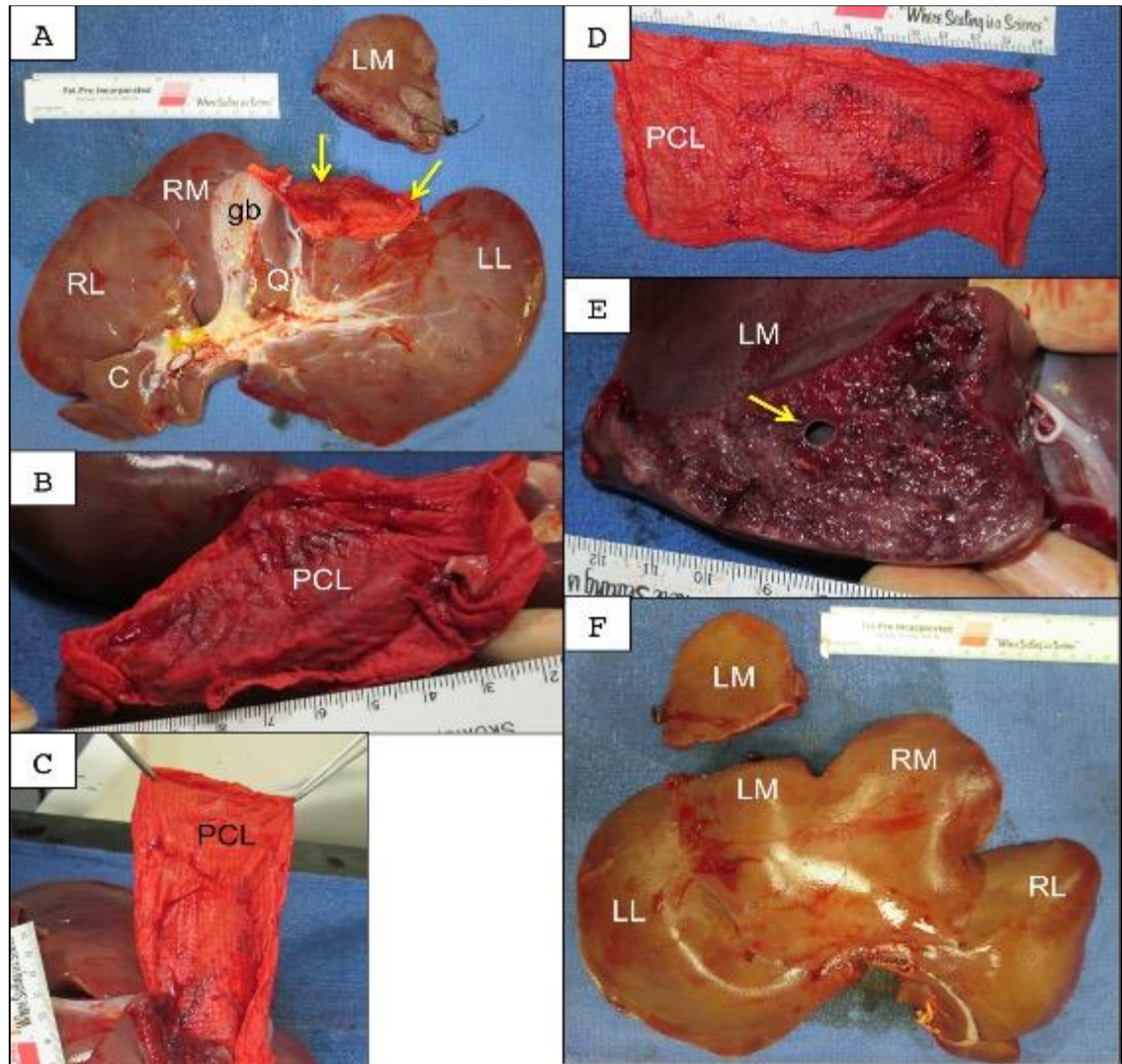


**Figure 9.** LM lobe resection & treatment with PCL+biologics and necropsy images. (A) Liver ex vivo specimen-inferior surface. Liver lobes: RL - right lateral, RM - right medial, LM - left medial, LL - left lateral, C - caudate lobe, Q - quadrate lobe, gb - gallbladder, arrows indicating injury site. (B) Injury site with PCL mesh close-up. (C) PCL mesh peeled off from injury site. (D) PCL mesh from necropsy. (E) Close-up of injury site, arrow pointing a transected hepatic vein. (F) Liver ex vivo specimen-superior surface, abbreviations same as fig A



The blood samples were sent for analysis to the clinical laboratory of the VA Medical Center in Omaha, Nebraska. Hematological assays included complete blood count, serum lactate, arterial blood gas analysis, liver function tests and complete coagulation profile were measured. [47, 48] The complete coagulation profile measures prothrombin time (PT), international normalized ratio (INR), activated partial thromboplastin time (PTT), and plasma fibrinogen. [47, 48]

### Statistical Analysis

Multiple comparisons between the groups were performed by paired t-test (for paired groups of data over time) or ANOVA (for unpaired groups of data at a single time point). All statistical analyses were performed with GraphPad Prism 7.0 software. Data are presented as mean  $\pm$  standard deviation. *P* values of  $<0.05$  will be considered significant.

## **2.3 Results**

Fifty-one Yorkshire random-bred pigs were randomized into 4 different treatment groups. One anesthetic death occurred in group 3, leaving 50 subjects for analysis. For simplification purposes, the group 1 consisted of animals whose grade V liver injury was treated with cautery, suture ligation and Surgicel® application. This group was referred as “control-group”; group 2, consisted of the second set of animals who were treated with polycaprolactone (PCL) mesh alone (16cm x 8cm, six-ply) were referred as “PCL-group”; group 3 had animals whose injury was treated with PCL mesh and fibrin sealant (combination of human plasma-derived fibrinogen (pdFI), human recombinant thrombin (rFII) and human recombinant Factor XIII (rFXIII)) and was named as the “fibrin sealant-group” ; and finally group 4 animals were treated with PCL mesh supplemented with rFII



and rFXIII only, was referred to as the “biologics-group”. The pre-injury parameters like pre-injury heart rate, pre-injury mean arterial pressure, pre-injury hemoglobin, pre-injury hematocrit, pre-injury prothrombin time, pre-injury INR, pre-injury PTT, pre-injury fibrinogen, pre-injury platelet count, pre-injury blood loss, and pre-injury fluid administration, were not statistically different among the four treatment groups (Table 1).

**Table 2.** Comparison of baseline animal characteristics among different groups

Variable	Control-Group	PCL-Group	Fibrin Sealant-Group	Biologics-Group	p-value
Number	12	14	13	11	N/A
Weight (kg)	36.6 ± 3.6	36.9 ± 3.1	40.6 ± 8.4	35.9 ± 3.1	0.134
Spleen mass (g)	313.3 ± 70.9	311 ± 51.1	338.6 ± 104.9	281.5 ± 77.5	0.376
Post-splenectomy replacement fluid (ml)	1093.1 ± 289.3	1025.5 ± 226.6	1059.6 ± 341.4	856 ± 227	0.192
Preinjury blood loss (ml)	358 ± 84.8	365 ± 50.7	381 ± 131.6	309.5 ± 78.5	0.277
Preinjury MAP (mm Hg)	113 ± 14	114 ± 22	113 ± 13	106 ± 6	0.247
Hematocrit (%)	37.7 ± 2.4	39 ± 3.7	39 ± 4.6	39 ± 1.5	0.110
Hemoglobin (g/dl)	11.2 ± 0.7	11.4 ± 0.9	12 ± 0.7	11.6 ± 0.4	0.070
Platelets (1000/ul)	400 ± 108	264 ± 60	293.4 ± 111	417 ± 104	0.06
PT (s)	11 ± 0.9	10.7 ± 0.9	11 ± 0.7	11 ± 0.4	0.930
INR	0.9 ± 0.06	0.95 ± 0.07	0.95 ± 0.05	0.95 ± 0.05	0.668
Fibrinogen (mg/dl)	107 ± 21	111 ± 22	102 ± 15	123 ± 16	0.011

Data = Mean ± SDV; PT-prothrombin time; INR-international normalized ratio

**Table 3.** Comparison of animal characteristics 10-min Post-Injury among different groups

Variable	Control-Group	PCL-Group	FS-Group	Biologics-Group	p-value
Number	12	14	13	11	N/A
Injury blood loss (ml)	267.3 ± 152.3	181.7 ± 164.6	333.6 ± 226.7	97.4 ± 73.8	0.277
Injury MAP (mm Hg)	82.7 ± 14.6	96.5 ± 23.5	72.2 ± 28.2	81.4 ± 9.8	0.247
Hemoglobin (g/dl)	11.53 ± 1.2	12.3 ± 1	11.3 ± 1.2	12.1 ± 1	0.070
Hematocrit (%)	38.64 ± 4.11	41.6 ± 3.4	37.9 ± 3.7	41.5 ± 5.7	0.110
Platelets (1000/ul)	369.4 ± 83.3	284.7 ± 63.5	268.5 ± 102.8	314.5 ± 114	0.06
PT (s)	10.5 ± 0.9	11.2 ± 0.8	10.9 ± 0.8	10.68 ± 0.6	0.930
INR	0.92 ± 0.09	0.96 ± 0.08	0.95 ± 0.07	0.93 ± 0.06	0.668
Fibrinogen (mg/dl)	83.08 ± 16.9	101.9 ± 13.5	90.8 ± 14.8	112.7 ± 17.86	0.011

Data = Mean ± SDV; PT-prothrombin time; INR-international normalized ratio

In all the treatment groups, all animals achieved hemostasis and survived the 1-hour monitoring period. Hemostasis was achieved within the first five minutes of bimanual compression in majority of the animals across all the treatment group. Hemostasis was confirmed at the 1-hour post-compression inspection of the intraabdominal cavity. Mean injury blood loss, injury MAP, injury mean hemoglobin, injury hematocrit, injury Platelets, injury prothrombin-time, INR and injury plasma fibrinogen level at 10 mins post-injury were not significantly different among all treatment groups.

**Table 4.** Comparison of animal characteristics 60-min Post-Injury among different groups

Variable	Control-Group	PCL-Group	FS-Group	Biologics-Group	p-value
Number	12	14	13	11	N/A
Injury blood loss (ml)	318 ± 137	314 ± 224	563 ± 387	161 ± 77	0.004
Injury MAP (mm Hg)	81 ± 14	88 ± 25	80 ± 20	75 ± 14	0.608
Hemoglobin (g/dl)	11.4 ± 1.5	11.9 ± 1.0	11.2 ± 1.4	11.9 ± 1.3	0.523
Hematocrit (%)	38.64 ± 4.11	41.6 ± 3.4	37.9 ± 3.7	41.5 ± 5.7	0.110
PT (s)	10.4 ± 1.2	10.7 ± 0.8	11 ± 0.9	10.4 ± 0.8	0.430
INR	0.92 ± 0.09	0.96 ± 0.08	0.95 ± 0.07	0.93 ± 0.06	0.668
Fibrinogen (mg/dl)	82.9 ± 18.3	97.9 ± 12.6	88.7 ± 13.8	110.9 ± 19.3	0.04

Data = Mean ± SDV; PT-prothrombin time; INR-international normalized ratio

Twelve animals were tested in group 1. All the animals tolerated the procedure and survived the 60 min observation period with an average 60 min MAP of  $81 \pm 14$  mm Hg. Mean post-injury blood loss was  $318 \pm 137$  ml, hemoglobin was  $11.4 \pm 1.5$  g/dL, final pro-time was  $10.4 \pm 1.2$  s and final fibrinogen level was  $82.9 \pm 18.3$  mg/dL. Upon evaluation during necropsy, the injury site was sealed, and the explanted liver specimen had at least 1-2 hepatic veins and 1-2 portal veins lacerated. This treatment group functioned as a positive control.

Fourteen animals were tested in group 2 or the "PCL only" treatment group. All the animals tolerated the procedure and survived the 60 min observation period with an average 60 min MAP of  $88 \pm 25$  mm Hg. Mean post-injury blood loss was  $314 \pm 224$  ml, hemoglobin was  $11.9 \pm 1.0$  g/dL, final pro-time was  $10.7 \pm 0.8$  s and final fibrinogen level was  $97.9 \pm 12.6$  mg/dL. Upon evaluation during necropsy, the injury site was sealed, and the explanted liver specimen had at least 1-2 hepatic veins and 1-2 portal veins lacerated.

Thirteen animals were tested in group 3 or the "PCL+FS" treatment group. One animal expired due to an anesthetic complication. All the other animals tolerated the procedure and survived the 60 min observation period with an average 60 min MAP of  $80 \pm 20$  mm Hg. Mean post-injury blood loss was  $563 \pm 387$  ml, hemoglobin was  $11.2 \pm 1.4$  g/dL, final pro-time was  $11 \pm 0.9$  s and final fibrinogen level was  $88.7 \pm 13.8$  mg/dL. Upon evaluation during necropsy, the injury site was sealed, and the explanted liver specimen had at least 1-2 hepatic veins and 1-2 portal veins lacerated.

Eleven animals were tested in group 4. All the animals tolerated the procedure and survived the 60 min observation period with an average 60 min MAP of  $75 \pm 14$  mm Hg. Mean post-injury blood loss was  $161 \pm 77$  ml, hemoglobin was  $11.9 \pm 1.3$  g/dL, final pro-time was  $10.4 \pm 0.8$  s and final fibrinogen level was  $110.9 \pm 19.3$  mg/dL. Upon

evaluation during necropsy, the injury site was sealed, and the explanted liver specimen had at least 1-2 hepatic veins and 1-2 portal veins lacerated.

In conclusion, blood loss was different among groups, with group 3 and 4 having the highest and lowest blood loss, respectively. Final plasma fibrinogen level also was different, with group 4 having the highest. Final MAP, final Hemoglobin and final prothrombin time were not different among the groups.

## *2.4 Discussion*

The PCL bandage-only and PCL + biologics categories were not different from the control group in terms of blood loss, mean arterial pressure readings, heart rate, hemoglobin, hematocrit and coagulation profile. Although the PCL + Fibrin Sealant group suffered a larger amount blood loss when compared to all the other treatment categories, their vital signs and coagulation profile was no different. In conclusion, the resorbable PCL mesh, either alone or in combination with rFII + rFXIII, appeared to have equivalent or better hemostatic efficacy (with respect to post-injury blood loss) compared with traditional surgical technique in this model of porcine hepatic resection.

Fibrinogen or factor I is one of the most critical coagulation factors for the formation of blood clot. [52] Normal circulating plasma fibrinogen level in humans is 200-400mg/dL and the levels increase with age. [52] Normal porcine circulating levels of fibrinogen is 120-200 mg/dL. [53] Baseline fibrinogen level in this experimental set up amongst all the study groups ranged from  $102 \pm 15$  mg/dl to  $123 \pm 16$  mg/dl. Baseline fibrinogen level was the highest in the biologics group at  $123 \pm 16$  mg/dl to begin with. 10-minutes post-injury the fibrinogen level decreased by about 12-15% the baseline with the highest level still in the biologics group at  $112.7 \pm 17.86$  mg/dl. There was no significant difference amongst the different experiment group at 10 minutes post-injury.

60- minutes post-injury the fibrinogen level decreased by only by about 1-2% from 10-min post injury level with the highest level still in the biologics group at  $110.9 \pm 19.3$  mg/dl. The fibrinogen levels in the control-group differed significantly from the biologics at 60 minutes post-injury. Based on the fact that the pigs in biologics group started with a high baseline fibrinogen level and the percent decrease in fibrinogen level amongst each group at 10-minute and 60-minute post injury interval was very similar, the final difference in the fibrinogen level between the control-group and biologics-group likely does not bear any clinical significance.

We believe, the swine models of non-compressible hemorrhage closely parallel the human non-compressible hemorrhage situations as they have similar anatomic, physiologic and biochemical characteristics. Young domestic Yorkshire pigs around the age of 3-5 months are reasonably large (35 – 45 kg) with a comparable liver mass (1.2-1.6 kg) blood volume of 2.6L as humans which makes them ideal candidates for large animal studies. [54] Yorkshire pigs were chosen because of their easy availability, maintenance and easy manual handling. Because of the small size and small blood volume small animal models of non-compressible hemorrhage (e.g., rodents and rabbits) may not produce a clinically relevant data.

Previously our laboratory has developed and demonstrated a hepatic left lateral lobe hemi-transection non-compressible hemorrhage model which produced an analogous 40% mortality when left untreated. [48] This is in congruous with the 50% mortality during the first 24 hours of trauma outcome. [25] It was clearly demonstrated during necropsy that the explanted liver on an average had 1 portal vein branch and 1 hepatic vein branch transected. In this study we chose a hepatic left medial lobe hemi transection non-compressible hemorrhage model, to demonstrate the efficacy of the PCL bandages. Like the hepatic left lateral lobe hemi transection models the hepatic left

medial lobe hemi transection model demonstrate hepato-venous and porto-venous injury.

A strength to this study was that the same surgeon performed the excision of the left medial lobe of the liver, applied the treatment gauze and applied the similar bimanual compression to reduce inter-personnel variation. In addition, the treatment groups were randomized using an electronic software increasing the confidence in the outcome.

Although this is proven to be a reliable model of non-compressible hemorrhage, there may be some limitations associated with this study that needs to be addressed in the future. Firstly, the battlefield and accident associated traumatic injuries may be far more complex than utilized in this study. Secondly, the efficacy of the bandages could be affected by wound conditions and the mode of application of biologics. Lastly, a larger sample size may have produced a different result. The next step in these studies will involve long-term toxicity trials in a larger sample of domestic swine.

## CHAPTER 3

### Porcine Model of Hindlimb Ischemia

*Some of the materials presented in this chapter has been published: Y Gao, S Aravind, NS Patel, M Fuglestad, JS Ungar, CJ Mietus, S Li, GP Casale, II Pipinos, MA Carlson. “Collateral Development and Arteriogenesis in Hindlimbs of Swine After Ligation of Arterial Inflow”. J Surg Res. 2020 May; 249:168–179, doi: 10.1016/j.jss.2019.12.005 PMID: PMC7218255*

#### 3.1 Introduction

Peripheral Vascular Disease (PVD) is a chronic arterial disease characterized by blockage or narrowing of the peripheral arterial system of the lower extremities. [55-58] Peripheral Vascular Disease (PVD) affects nearly 10 million people in United States making it a major economic burden to the country. [55-58] The prevalence of Peripheral Vascular Disease (PVD) is increasing rapidly especially among the developing countries. [55-58] It is a disease of the elderly and relatively uncommon in younger population. [55-58] Peripheral Vascular Disease (PVD) is associated with significant morbidity and mortality with clinical complaints ranging from atypical leg pain, chronic ulcers, intermittent claudication to threatened limb caused by Critical Limb Ischemia (CLI). [55-58] More than 50% of PVD patients are asymptomatic and associated with multiple co-



morbidities. [55-58] Nearly 20-30% of the individuals with PAD have diabetes mellitus. [55-58] Patients with diabetes and PVD combined have a 2-6-fold higher chance of mortality from Coronary Artery Disease (CAD). [55-58] Thus, the first line treatment of Peripheral Vascular Disease (PVD) is optimal medical management of co-morbidities like diabetes mellitus, hypertension, hyperlipidemia and reducing the risk of any cardiovascular event. [55-58] The only FDA approved medication for treating the symptoms of Peripheral Vascular Disease (PVD) is cilostazol, which is proven to have minimal benefit to this patient population. [55-58]

A severe form of PAD associated with chronic obstruction of blood supply to the limb, wherein the viability of the limb is threatened is called critical limb ischemia (CLI). [55-57, 59, 60] Critical limb ischemia is characterized by inadequate tissue vascularization causing reduced perfusion and tissue oxygenation resulting in ulceration, gangrene or infection. [59, 60] The diagnosis of CLI is made when the Ankle Brachial Index is  $<0.4$  and or the Toe Brachial Index is  $<0.3$ . [59, 60] If left untreated, CLI is associated with 20% mortality within 6 months and 50% at 5 years of diagnosis. [55-57, 59, 60] Treatment option for CLI is either open/surgical or endovascular revascularization procedures, however approximately 25-40% of these chronic ischemia patients end-up having amputation of the non-viable limb. [59, 60] The annual mortality in this patient population is about 20%. [56, 59, 60]

Currently treatment for PVD is limited to lifestyle modifications and optimization of medical co-morbidities with or without surgical or endovascular revascularization procedures. [55, 56, 60, 61] Upto 30% of these patients may not qualify for endovascular or surgical revascularization procedures. [55, 56, 58] It is important to constantly develop novel medical and surgical therapies for the treatment of PAD and CLI. A well-characterized, large animal model can be extremely valuable in the study of

PAD and CLI. [62] A large animal model of PVD can be used to design and implant peripheral arterial stents and at the same time can be used to test out different medical and regenerative strategies. [62]

### Specific Aim.

In this project we propose to develop a novel porcine model of end-organ disease for peripheral arterial atherosclerosis, in order to have a platform to develop and optimize regenerative therapies.

### Hypothesis.

We hypothesize, that this novel swine model of hindlimb ischemia will induce acute ischemia in the treated limb leading to ischemic changes in the muscle similar to the myopathy of peripheral arterial disease seen in human counterparts.

### Terminology.

Before discussing the methodology and the different strategies that have been evaluated in this model, following is the brief introduction of the different terminology that has been used in this chapter.

- 1) Angiogenesis - True angiogenesis is the formation of de novo capillaries in response to tissue hypoxia, and or ischemia. [62, 63] In response to hypoxia, growth factors such as Vascular Endothelial Growth Factors (VEGF) and Hypoxia Inducible Factor - 1(HIF-1) are released leads to growth of new capillary network. [62, 63] This process is complete within few days. [64]
- 2) Arteriogenesis - Arteriogenesis is a process by which preformed or pre-existing collaterals formed during embryogenesis are recruited when there is acute or chronic occlusion of the of medium or large artery. [62, 63] Acute or chronic

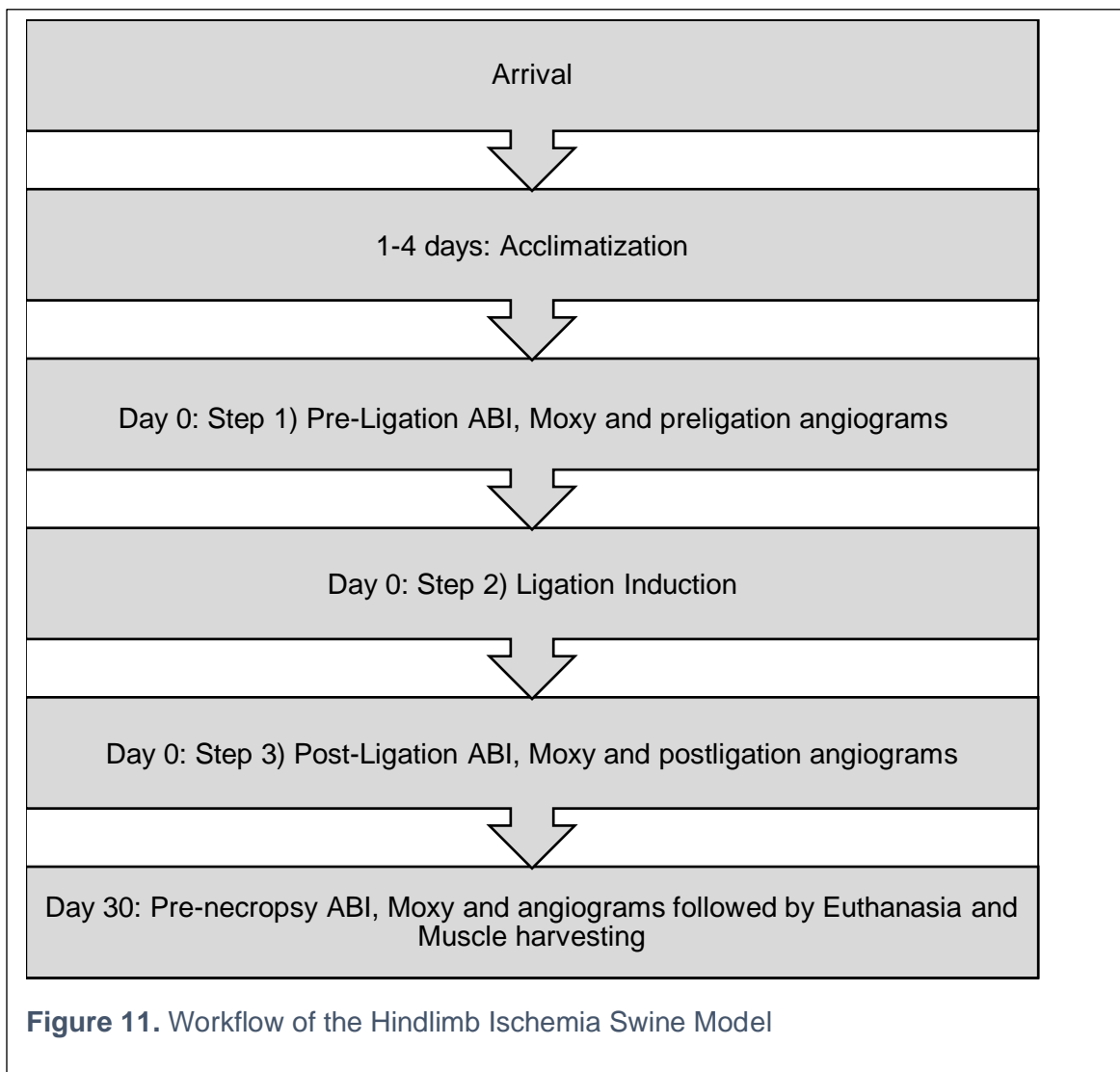
blockage of arteries leads to shear stress leads to upregulation of proteins like Nitric Oxide Synthase (NOS) and Platelet Derived Growth Factor (PDGF) leading remodeling and recruitment of dormant small arteries and arterioles. [62] This process usually takes days to weeks to be complete. [64]

- 3) Vasculogenesis – During embryogenesis, development of initial vascular network (arteries, veins and capillaries) from angioblasts or vascular progenitor cells is termed vasculogenesis. [64, 65]
- 4) Collaterogenesis – Collaterals are naturally occurring bypass channels occurring between artery to artery or arteriole or arteriole which become active during an obstructive disease. [66] The process of development of collaterals during embryogenesis and early postnatal period. [66]

## *3.2 Materials and Methods*

### *Study Design*

This is a pre-clinical, non-human, exploratory study to develop a novel porcine model of end-organ disease for peripheral arterial atherosclerosis, in order to have a platform to develop and optimize regenerative therapies.



### Sample Selection

Since the swine models share similar anatomic, physiologic and biochemical characteristics with humans young domestic Yorkshire random-bred pigs were used in this study. Yorkshire pigs were chosen because of their easy availability and maintenance. Also, manual handling of the animals is easy when the animals are younger and smaller. Experimental animals for the study were in the age range of 3-5 months and were purchased from the Agricultural Research and Development Center (Mead, NE).

### Animal Welfare

Recommendation from National Institutes of Health detailed in the Guide for the Care and Use of Laboratory Animals (8th ed.) was used to ethically carry out all of the experimental procedures in this study protocol. [43] The animal protocol for the study was reviewed in detail and approved by the Institutional Animal Care and Use Committee of the VA Medical Center in Omaha, Nebraska. The VA Medical Center research facility is approved by Association for Assessment and Accreditation of Laboratory Animal Care International (AAALAC) and all procedures were performed in the AAALAC approved facilities. [43]

### Animal Preparation

We used, twenty-one Yorkshire random-bred commercial swine for the acute ischemia study and two Yorkshire random-bred commercial swine for the subacute ischemia study, all castrated males, aged ~3 months weighing 31-55 kg were brought from Agricultural Research and Development Center (ARDC) at Mead, Nebraska. Animals were housed indoors in individual cages under SPF (specific-pathogen free) conditions. During the 3-4-day acclimatization period, the animals had free access to water and were fed a corn and soybean based meal. [46]

### Induction and Anesthesia

Animals were fasted for at least 12 hours before the surgical procedure. [47] During this time, they had free access to drinking water. [47] Anesthesia induction for each animal was with a single 3 mL intra-muscular premixed cocktail injection containing 150 mg Telazol (Zoetis; 4.4mg/kg), 90 mg ketamine (Zoetis; 2.2mg/kg), and 90 mg xylazine (Zoetis; 2.2 mg/kg). [46] To minimize hypersalivation intramuscular atropine sulfate at a dose of 0.05 mg/kg was used on an as needed basis. Each animal was weighed and orotracheally intubated using a 7.0mm - 7.5 mm cuffed tube. [46] A peripheral line was placed in an auricular marginal vein as an additional access to administer fluids or medication. [34, 48, 49] Electrocardiogram monitor, buccal pulse oximeter and rectal temperature probe were placed. To maintain the body temperature at 37 C, animals were rested on a water-circulated heating pad. [34, 48, 49] Anesthesia was maintained with isoflurane (1%-2%) mixed with oxygen (1L-2L). [48] Throughout the procedure animals were mechanical ventilated in a pressure control mode delivering 13-15 breaths/minute, with a tidal volume of 5-10mL/kg, and the end-tidal partial pressure of CO<sub>2</sub> at 30–45 mm Hg. [34, 48, 49]. A single dose of cefovecin sodium (Zoetis; 8mg/kg intramuscular) and long-acting opioid analgesic were administered before the incision. [46]



**Figure 13.** Operative set up for swine procedures.

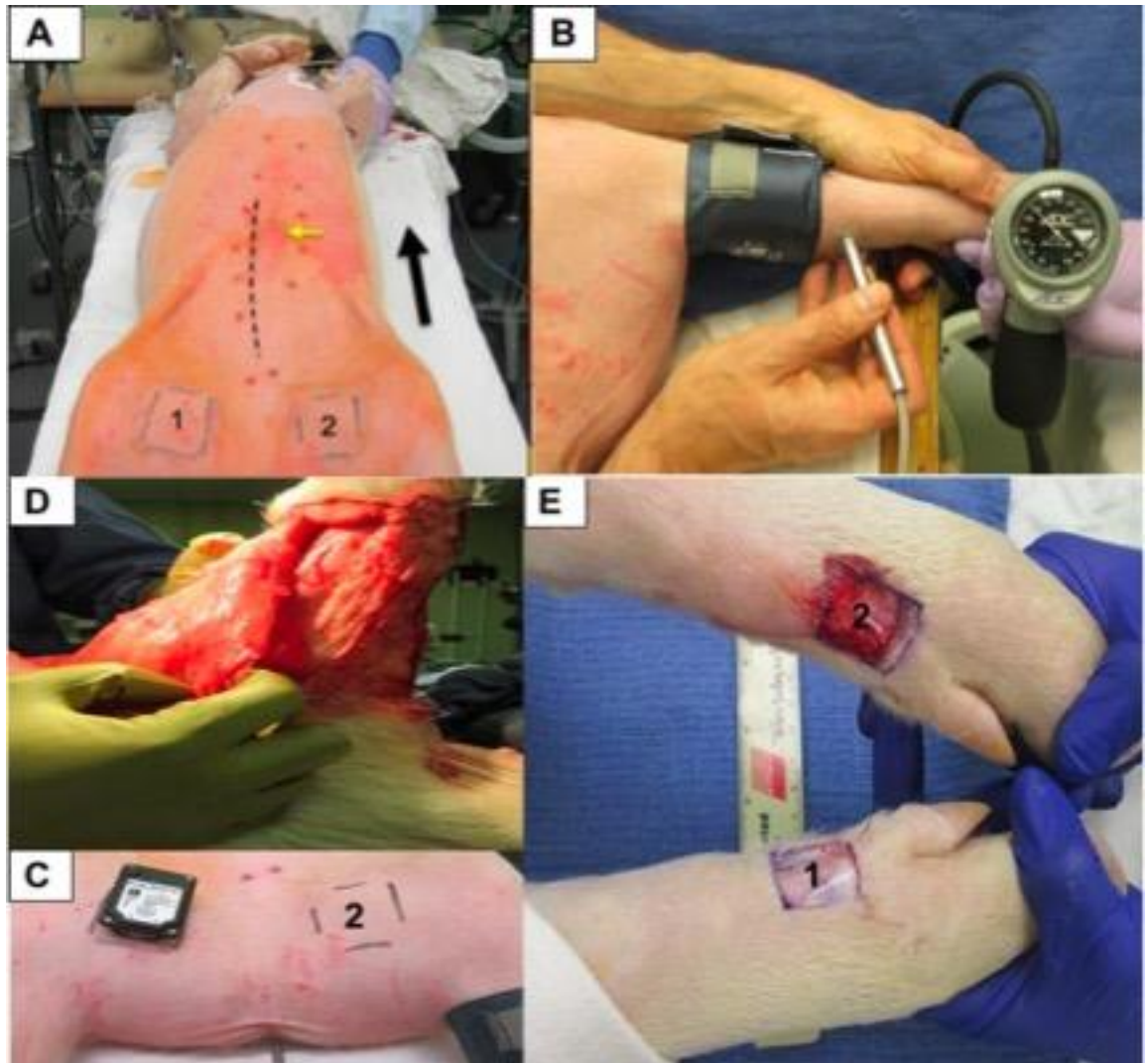


**Figure 15.** (A) Operative set-up. (B) Measurements of left hindlimb arterial pressure for ABI. (C) Moxy measurement on inner right thigh. (D) Muscle harvesting for histology, lateral head of gastrocnemius (E) 2cm x 2 cm full thickness excision of the skin on the medial aspect of bilateral hindlimbs (1) Ischemic limb and (2) Normal limb.

ABI-Ankle Brachial Index, Moxy-Muscle oximetry



### Initial Measurement

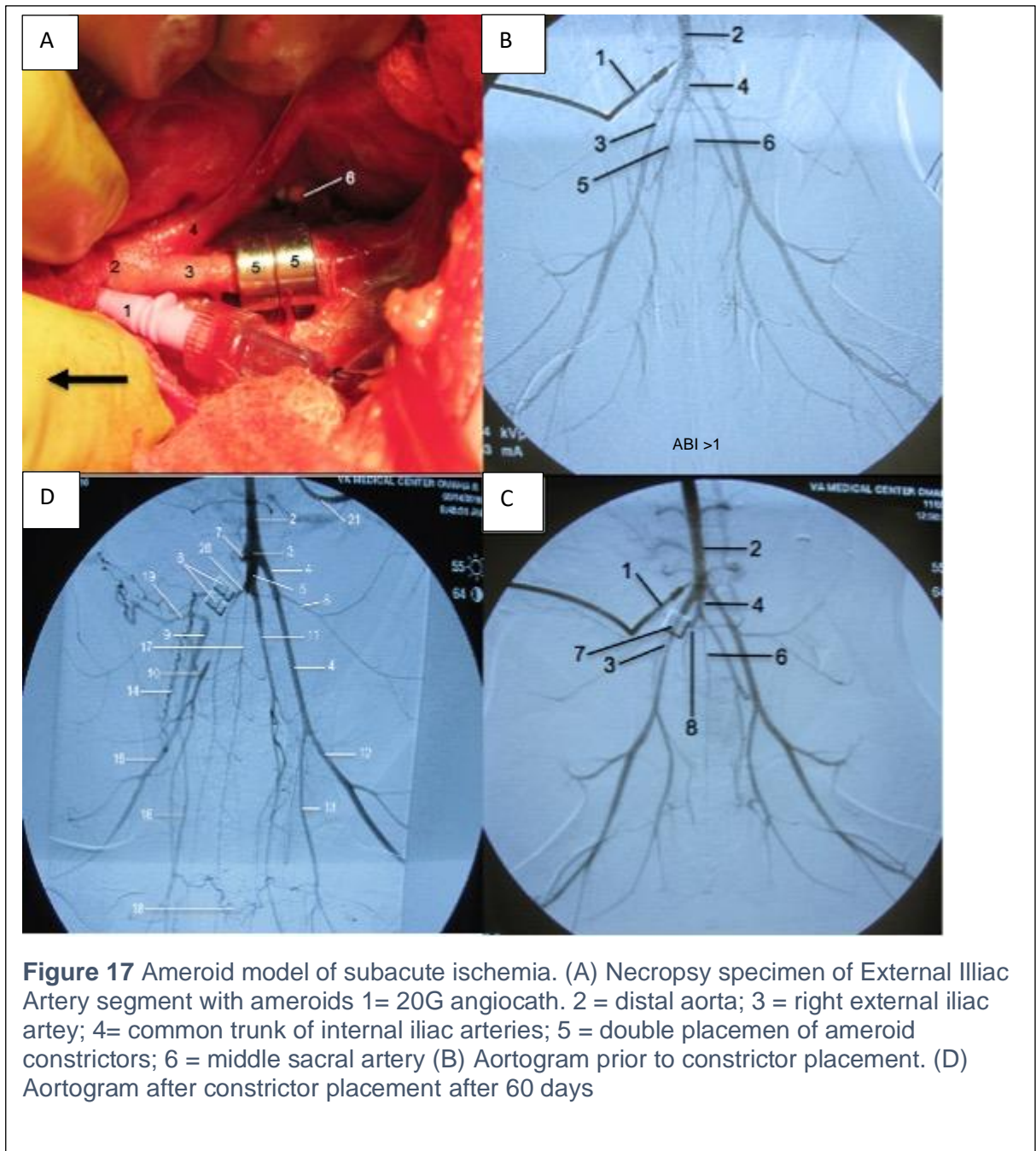
Ankle-Brachial Index is the ratio of systolic pressure of treated hindlimb to the systolic pressure of untreated hindlimb or forelimb. [55, 59-62] The initial limb blood pressure was performed using a handheld vascular doppler with a 3" cuff (fig 8 B). The systolic blood pressure (ABI) in bilateral forelimbs and hindlimbs was determined using standard techniques. [55, 59-62]

Muscle Oximetry is a non-invasive technique to measure muscle oxygen saturation using Near Infrared Spectroscopy (Moxy, Minnesota, USA). [67] It is the ratio of the oxyhemoglobin concentration to the total hemoglobin concentration. [67] It assesses the extent of tissue hypoxia or microcirculatory perfusion. [67] The Moxy device was laid flat on thick muscle belly in bilateral forelimbs and hindlimbs to measure the muscle tissue saturation recorded using real-time Moxy monitors (fig 8 A, C).

### Laparotomy and Aortograms

Under aseptic precautions, the animal's abdomen and groin were sterilely prepped and draped. [61] A ventral paramedian laparotomy incision was performed extending along the lower half of the abdomen. [61] The incision was then carried to the subcutaneous tissue and musculoaponeurotic layers using a bipolar cautery. [61] Peritoneum was then carefully dissected to enter a retroperitoneal space, to expose the abdominal aorta and its branches. [61] A 20-gauge angio-catheter was placed in the infrarenal portion of the aorta and secured in place using a 6-0 polypropylene U-stitch (see Fig. 9 A). [61] Serial angiograms were shot through this access throughout the procedure. [61] A baseline aortogram with runoff was obtained to determine any vascular abnormality before the ligation procedure which is explained under the next heading.

After the ligation procedure, a post ligation angiogram was performed, and the abdomen was closed in three layers and the skin closed with a 4-0 Vicryl suture. [61] The animal was monitored for approximately 4-6 hours in the recovery room and then transferred to their pens. [46]



### Ameroid model of subacute limb ischemia

The subacute hindlimb ischemia in this initial group (n=2) was created by placing a double 5mm Ameroid constrictors around the right external iliac artery (fig 9 A). [68, 69] An Ameroid constrictor is (fig 9 A) is made up of a hygroscopic casein ring encased in a stainless-steel sheath. [68, 69] Casein ring slowly absorbs bodily fluid and swells up while the stainless-steel encasing forces the casein ring to close inwardly over a period of 4-5 weeks. [68, 69] Both the size of the vessel and the Ameroid constrictor determines the time of occlusion of the vessel. [68, 69]

Simultaneous right internal arteriotomy was performed. Repeat Aortograms, ABIs and muscle oxygen saturations were performed immediately after the procedure and 60 days post-operatively right before necropsy (fig 3D).

The Ameroid model of subacute ischemia produced a mild-moderate peripheral vascular disease as evidenced by the marginally decreased ABI and angiogenesis but failed to produce any myopathy. Hence this line of experimentation was aborted.

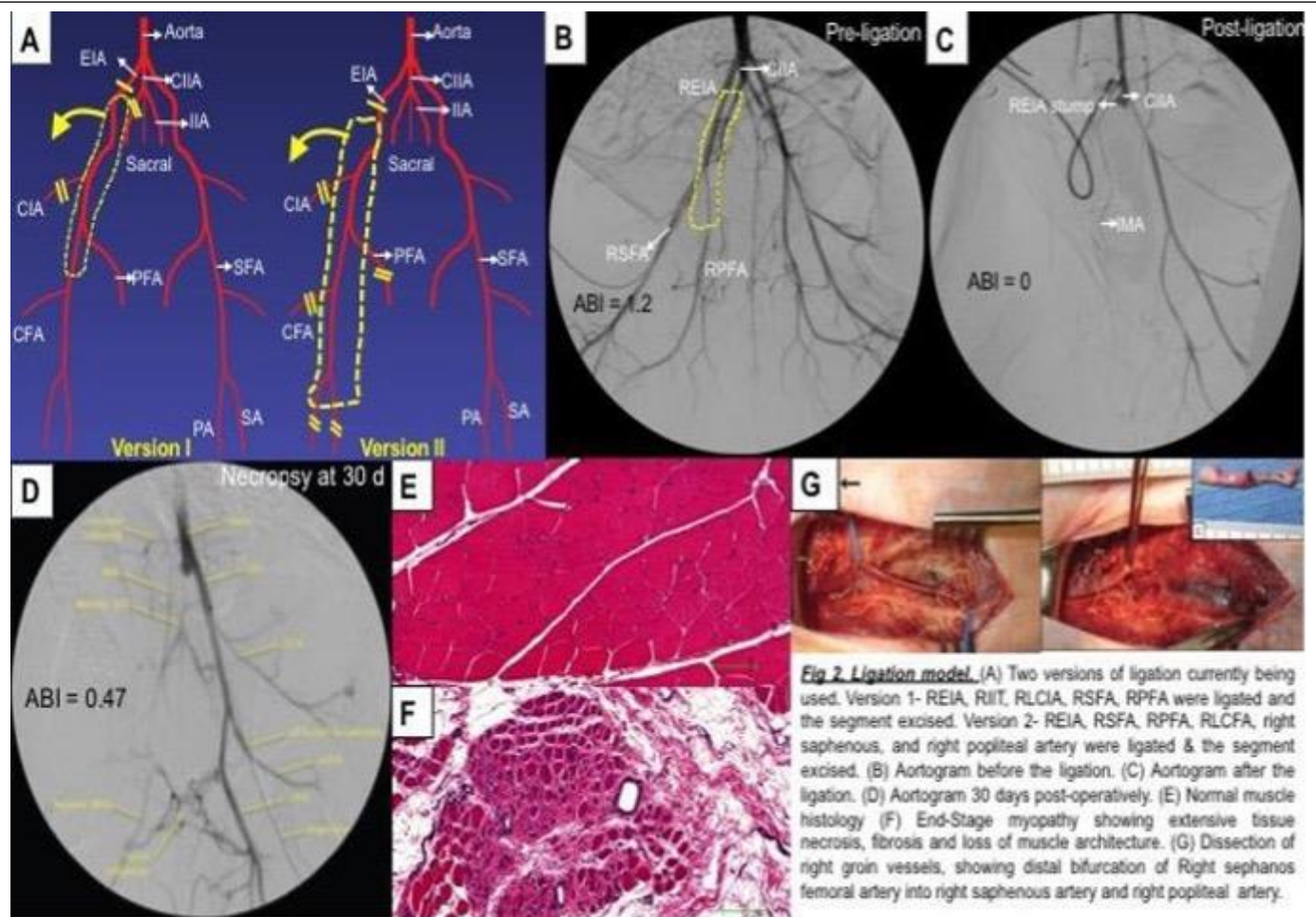


**Figure 19** Ligation model of acute ischemia. (A) Two versions of ligation, Version 1 – REIA, RIIT, RLCFA, RSFA, RPFA were ligated, and segment excised, Version 2 – REIA, RSFA, RPFA, RLCFA, RSA AND RPA arteries were ligated. (B) Aortogram before the ligation (C) Aortogram after the ligation. (D) Aortogram 30 days post-operatively. (E) Normal muscle histology. (F) End-Stage myopathy. (G) Dissection of the groin vessels.

REIA - Right external iliac artery, RIIA - Right Internal iliac artery, RLCFA – Right Lateral Circumflex Femoral Artery, RSFA - Right saphenofemoral artery, RPFA - Right profunda femoral artery, RSA- Right saphenous artery, RPA- Right popliteal artery

Ligation model of acute limb ischemia [61]

Hindlimb ischemia was induced acutely by segmental excision of the right external iliac artery, right circumflex iliac artery, right profunda femoris artery, right superficial femoral artery, right circumflex femoral artery, right popliteal artery and right saphenous artery. Subjects were then randomized roughly into two groups 1) *Version 1*- without right internal iliac artery (RIIA) ligation and 2) *Version 2*- with right internal iliac artery (RIIA) ligation. Repeat Aortograms, SBPs & muscle oxygen saturations were performed immediately after the procedure and 30days post-operatively. In addition, subjects with version 1 ligation were walked on a motorized treadmill at a constant speed to test the maximum walking potential before and 30days after the ligation procedure.

### Euthanasia and Necropsy

At the end of 30-day observation period after the ligation procedure, animals were sedated and orotracheally intubated using standard procedures. [51] ABIs and muscle oxygen saturation were measured in all four limbs using the same standard technique mentioned above. Using Seldinger technique, left common carotid artery was cannulated, through which a catheter was advanced into the abdominal aorta and serial aortograms with run offs were then performed for the evaluation of abdomino-pelvic and extremity circulation. Multiple oblong biopsies of bilateral muscle bellies of gastrocnemius and soleus are taken and transported in methacarn to University of Nebraska Medical Center for fixation and processing. The isoflurane inhalation was then increased to 5%. [51] At the end of 5 minutes of isoflurane induction, the diaphragm was then incised attempting to expose the inferior vena cava which is then transected, to let the animal bleed, [51] which is in accordance with AVMA Guidelines. [51] According to AVMA guidelines , death is as MAP <10 mm Hg with no identifiable pressure wave tracing. [51]

### Bright-field microscopy

Porcine muscle specimens were processed at a collaborative laboratory at University of Nebraska Medical Center.

### Endpoints

Ankle-Brachial Index- detects and quantifies peripheral arterial disease. [55-57, 60] It is the ratio of systolic pressure of treated hindlimb to the systolic pressure of untreated hindlimb or forelimb. [55-57, 60]

Muscle Oxygen Saturation- measures the extent of tissue hypoxia/microcirculatory perfusion. [67] Moxy measures muscle oxygenation which is the ratio of the oxyhemoglobin concentration to the total hemoglobin concentration. [67]

Aortograms with run-offs- Terminal arteriography helps to study and measure the reconstitutions and collateralization of the ligated vessels. [61]

Maximum treadmill walk time- compares the exercise potential before and after the ligation procedure.

Muscle histology- Multiple bilateral tissue samples from major and minor hindlimb muscle groups were obtained to study the extent of ischemic myopathy & regeneration. Ischemic myopathy is quantified by both manual and automated procedures. [61]

### Statistical Analysis

Multiple comparisons between the groups were performed by paired t-test (for paired groups of data over time) or ANOVA (for unpaired groups of data at a single time point). All statistical analyses were performed with GraphPad Prism 7.0 software. Data are presented as mean  $\pm$  standard deviation. *P* values of  $<0.05$  will be considered significant.



### 3.3 Results

**Table 5.** Endpoint measurement for porcine model of chronic Hindlimb Ischemia.

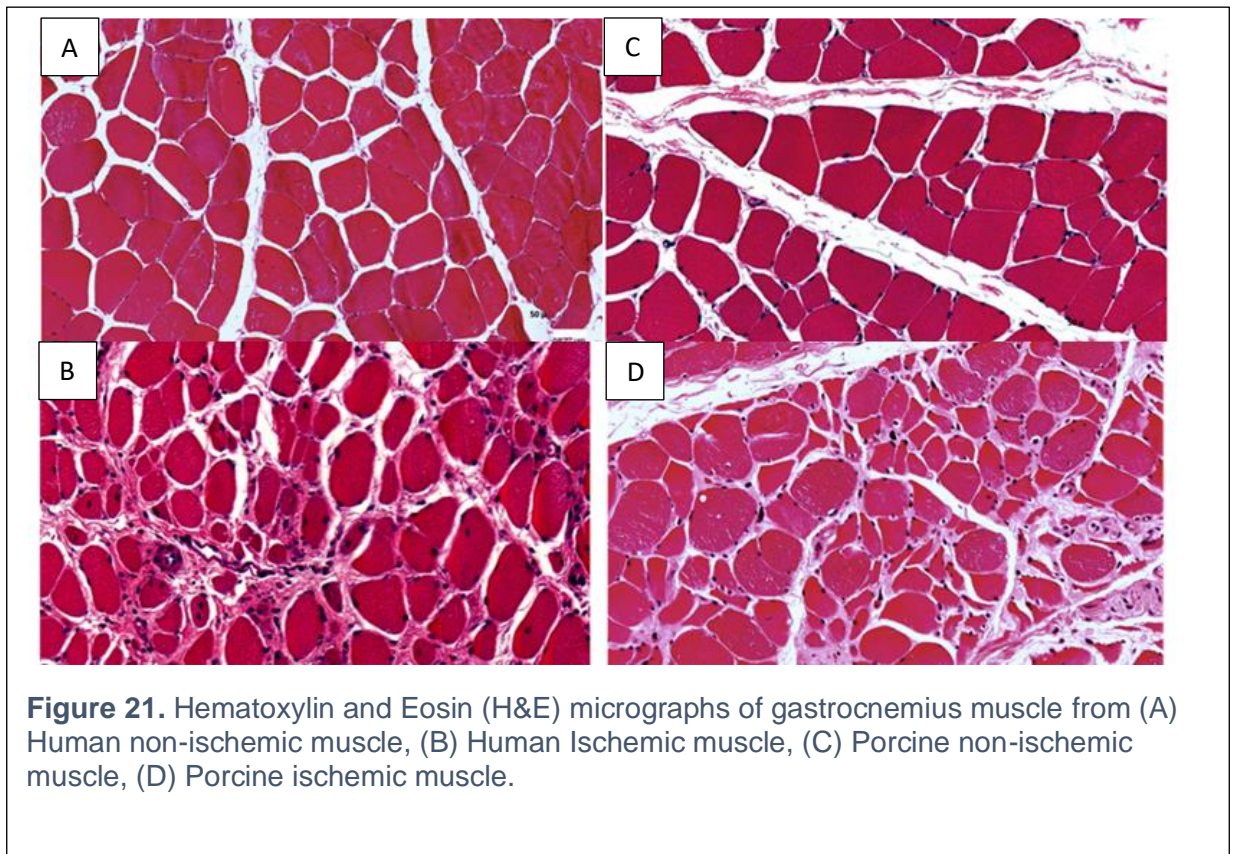
	Version 2/(+)RIIA ligation (N = 10)						
	t = 0, Pre		t = 0, Post		Final		
Endpoint	Right	Left	Right	Left	Right	Left	P-value
SBP	124.9±24.1	119.7±18	0±0	119.4±36.6	47±34.3	118.2±25.8	<0.001
Mb Sat (%)	57.2 ±12.8	57±13.6	18±4.2	45±8.5	33.1±11.8	53.6±9.6	<0.001
Max TT (min)	NR	NR	NR	NR	NR	NR	NR
MS (0-4)	NR	NR	NR	NR	4	1	< 0.0001

	Version 1/(-)RIIA Ligation (N = 11)						
	t = 0, Pre		t = 0, Post		t=30, Final		
Endpoint	Right	Left	Right	Left	Right	Left	P-value
SBP	102.4±26.7	107±29.8	0±0	97.5±17.4	65.6±30.9	112.1±20.3	<0.001
Mb Sat (%)	64.7±16.3	68.6±15	24±7.4	53.9±12.6	43.9±14.6	63.5±11.4	<0.001
Max TT (min)	31.7±0.6	NR	0±0	NR	9.7±11	NR	<0.05
MS (0-4)	NR	NR	NR	NR	2	1	0.54

Pre = Prior to ligation; MOS: Mixed oxygen saturation, Post = Just after ligation; Final = Just prior to necropsy; NR= Nothing recorded; NA = Not applicable, \*ANOVA, within Method. MS: 0 = no myopathy; 1 = mild myopathy; 2 = moderate myopathy; 3 = severe myopathy; 4 = end-stage myopathy.

Twenty-one random bred Yorkshire pigs were used in this study. Eleven subjects in version 1 and 10 subjects in version 2 were used. The ABI (represented as SBP in the table 4 above) was calculated in both hindlimbs on day 0 (before ligation and immediately after ligation) and following this again on day 30 (before necropsy) (see Table 4). Post-injury SBP of the ischemic hindlimb (right side) were significantly lower than the normal hindlimb (left side) both immediately and 30 days after ligation procedure (Post -ligation acutely decreased SBP was acutely decreased to zero) (Table 4). Final SBP did not demonstrate any difference between the two versions of ligation.

Maximum treadmill walk time (Max TT) was significantly lower 30 days post-operatively among the version 1 subjects after the ligation procedure. Before necropsy, TT recovered to ~30% of the pre-ligation duration (data was only available for Method 1).



H&E micrographs of chronically ischemic gastrocnemius muscle (day 30, right hindlimb) versus control (contralateral) porcine gastrocnemius muscle are shown in Figure 11. The control muscle from both swine (Fig. 11) and humans (Fig. 11) demonstrated polygonal myofibers. Ischemic myopathy was quantified and scored manually based on presence of fibrosis and myofiber degeneration. The myopathy severity score for Method 2 was worse compared Method 1. In version 2 subjects myopathy score was significantly different between the ischemic and the normal limb, however it was not significantly different in version 1 subjects.

Post-Ligation, the day 30 angiography demonstrated consistent collateral development from the Right Internal Iliac Artery (RIIA) to profunda artery in Method 1, and from the lumbar arteries and Left Internal Iliac Artery (LIIA) to distal Right Internal Iliac Artery (RIIA) in Method 2.

### *3.4 Discussion*

Researchers have induced hindlimb ischemia in beagle dogs which are the only large animal models of ischemia in literature. [70, 71] Hindlimb ischemia in canine has been induced using two ways. One method is the open ligation method wherein the femoral artery and its branches are identified, dissected and ligated for the induction of hindlimb ischemia. [71, 72] The second method is to embolize femoral artery and its branches using an embolic agent (Polyvinyl alcohol embolic agent) or sclerosing agents using minimally invasive technique. [70] Induction of hindlimb ischemia in dogs has produced similar results as in pigs but when using canines as large animal models to mimic human diseases, researchers have to go through rigorous ethical hoops and the indications are very limited. [70] On the other hand, using pigs as large animal models

have less serious ethical implications due to it being the most populous mammal and the consumed animal for meat in the world. [7]

Based on the results obtained from systolic BP and muscle oxygen saturation, the two ligation versions induced ischemia both immediately post-ligation (day 0) and after the 30-day observation period. The two ligation versions were not significantly different from one another in terms of ABI (SBP) and muscle oxygen saturation. Also, induction of ischemia in the right hind limb did not affect the arterial pressure index or muscle oxygen saturation in the contralateral hind limb or the control limb. Maximum treadmill walk time (Tmax), was only performed on subjects who underwent version 2 ligation. There was no data available for treadmill time for version 1 ligation. The subjects who underwent version 1 ligation recovered to approximately 30% of pre-injury level which paralleled the collateral development in the ischemic limb. Myopathy score was an arbitrary score that was assigned based on the severity of ischemic features on the H&E micrographs, and these were assigned manually.

This is novel model of hindlimb ischemia, but it may be associated with some limitations that will need to be addressed in the future. Firstly, PAD is the disease of elderly, afflicting individuals with multiple co-morbidities which is in contrast with the animal subjects used in the study which are young pigs with no medical problems. Secondly, PAD is a chronic condition which usually takes years to develop and progress but our current model of hindlimb ischemia is more acute in nature and may not accurately represent the pathophysiology of the PAD mechanism. Lastly, use of Xray fluoroscopy in the study only produced low-resolution imaging but addition of computerized tomography images with higher resolution for the future resolution imaging

In conclusion, ligation and excision of the ilio-femoral complex in one hindlimb of the domestic swine produced a measurable difference in systolic blood pressure, muscle

oxygen saturation, and treadmill stamina, along with histological evidence consistent with ischemic myopathy similar to human counterparts. Further validation of this model is needed to demonstrate the reproducibility and correlation to human pathology.

## CHAPTER 4

### Porcine Model of Pancreatic Cancer

*Some of the materials presented in this chapter has been previously published as a preprint: Remmers N, Cox JL, Grunkemeyer JA, Aravind S, Arkfeld CK, Hollingsworth MA, Carlson MA. Generation of tumorigenic porcine pancreatic ductal epithelial cells: toward a large animal model of pancreatic cancer. bioRxiv (preprint). 2018; doi:10.1101/267112.*

*Some of the materials presented in this chapter has been published as a preprint: Patel NS, Bailey K, Lazenby AJ, Carlson MA. Induction of pancreatic neoplasia in the KRAS/TP53 Oncopig. bioRxiv (preprint). 2020; doi: 10.1101/2020.05.29.123547*

#### 4.1 Introduction

In United States and worldwide, the incidence of Pancreatic Cancer (PC) is rapidly increasing since the 1990s. [73, 74] According to SEER (Surveillance, Epidemiology, and End Results) statistics, pancreatic cancer is the 11<sup>th</sup> most common cancer and fourth most common cause of cancer related deaths in United States. [75, 76] According to NIH cancer statistics in 2020, there were nearly 57,600 new cases of pancreatic cancer and nearly 46,000 new deaths because of pancreatic cancer. [75, 76] The overall 5-year survival for pancreatic cancer is <10%. [73-76] Per 2016 SEER

(Surveillance, Epidemiology and End Result) data the 5-year survival rate for localized, regional and distant disease were 39.3%, 13.3% and 2.9% respectively. [76] Thus, there is a need for improvement in pancreatic cancer diagnosis and management. [77]

Pancreatic adenocarcinoma which accounts for more than 90% of pancreatic cancer arises from the ductal epithelium. [73, 74] Most common genetic alterations in pancreatic ductal adenocarcinoma are the *KRAS*, *TP53*, *CDKN2A*, *SMAD4*, *BRCA1*, and *BRCA2* genes. [78] Historically, to develop new therapies for pancreatic cancer, genetically engineered mice are commonly used in preclinical testing. [1, 17, 79] However, murine models may not accurately reflect tumor heterogeneity, architecture, response to drugs, and other characteristics that are observed in human tumors. [2, 3, 6, 8, 15] In addition, differences in overall size, metabolism, and pharmacokinetics between mice and humans have limited the utility of murine models in the development and validation of novel anti-cancer therapies. [2-4, 6, 10, 15] Of note, the porcine-human genome has a greater homology compared to the murine-human homology. [6] As a model organism in biomedical research, pigs generally are a better mimic of humans than are mice with respect to anatomy, size, physiology, metabolism, immune response, and genetic sequence. [5, 7, 9, 10, 19, 21, 22]

Recently, the feasibility of immunocompetent, genetically engineered porcine models of various cancers has been demonstrated. [80-83] There are several clear advantages that makes the pigs an ideal transitional model to study PC. Firstly, pigs attain sexual maturity at 6 months of age, have a short gestation period of about 4 months, produce an average of 10 piglets per litter and have an all-season breeding. [6, 8] While being expensive, experimental pig handling, housing, and monitoring have been standardized. [46] Secondly, like the primate animal models, pigs will produce a tangible resultant pancreatic tumor that can be used study imaging, radiation therapy and

photodynamic therapy. [11] Thirdly, tumorigenesis of porcine cells, is similar to human cancer and requires several genetic alterations and will make a highly predictive preclinical model to study anti-cancer therapies. [10, 20, 22, 81, 83] Finally, after standardizing the protocols, production of genetically engineered porcine PC model will be simple, rapid, easy and relevant to human PC. [84, 85]

In 2017, Schook et al. described a next generation transgenic minipig cancer model also known as the “Oncopig Cancer Model” (OCM). [80] Briefly, this research group initially isolated and cloned porcine *KRAS* and *TP53* genes. A site-directed mutation was then introduced at G12D and R167H to the *KRAS* and *TP53* genes respectfully. [80] The altered cDNA was then introduced into a palindromic Lox-Stop-Lox (LSL) sequence. [80] The LSL sequence is inhibitory to the expression of the cancer inducing transgenes until it is clipped by a Cre recombinase enzyme. [80] These transgenic pigs have been described by the same group to develop sarcoma, hepatocellular carcinoma etc. [86-88]

In this dissertation, we intend to develop a syngeneic porcine pancreatic cancer model using the Oncopig Cancer Model. A porcine model of PC will provide a platform to develop and study noninvasive imaging techniques and novel therapeutic drugs for clinical application. The size of the porcine subjects will permit studies on both diagnostic and therapeutic technologies that would otherwise be difficult in mice. In addition, a porcine model of pancreatic cancer likely would be more predictive of human response to novel anti-tumor therapies than the equivalent murine model.



## *4.2 Materials and Methods*

### *Study Design*

In this pre-clinical, large animal model of pancreatic cancer our goal was to induce pancreatic ductal adenocarcinoma in transgenic minipig, also known as Oncopig Cancer Model which will provide us with a novel large animal model to test diagnostic and therapeutic strategies.

### *Specific Aim.*

In this project we intent to develop a porcine pancreatic adenocarcinoma which will be large animal pancreatic cancer model to test diagnostic and therapeutic strategies.

### *Hypothesis.*

We hypothesize, that the injection of AdCre (Adenovirus carrying the Cre recombinase enzyme) into the pancreatic duct and the parenchyma of the transgenic Oncopig will produce tangible pancreatic ductal adenocarcinoma expressing cancer specific molecular and genetic markers.

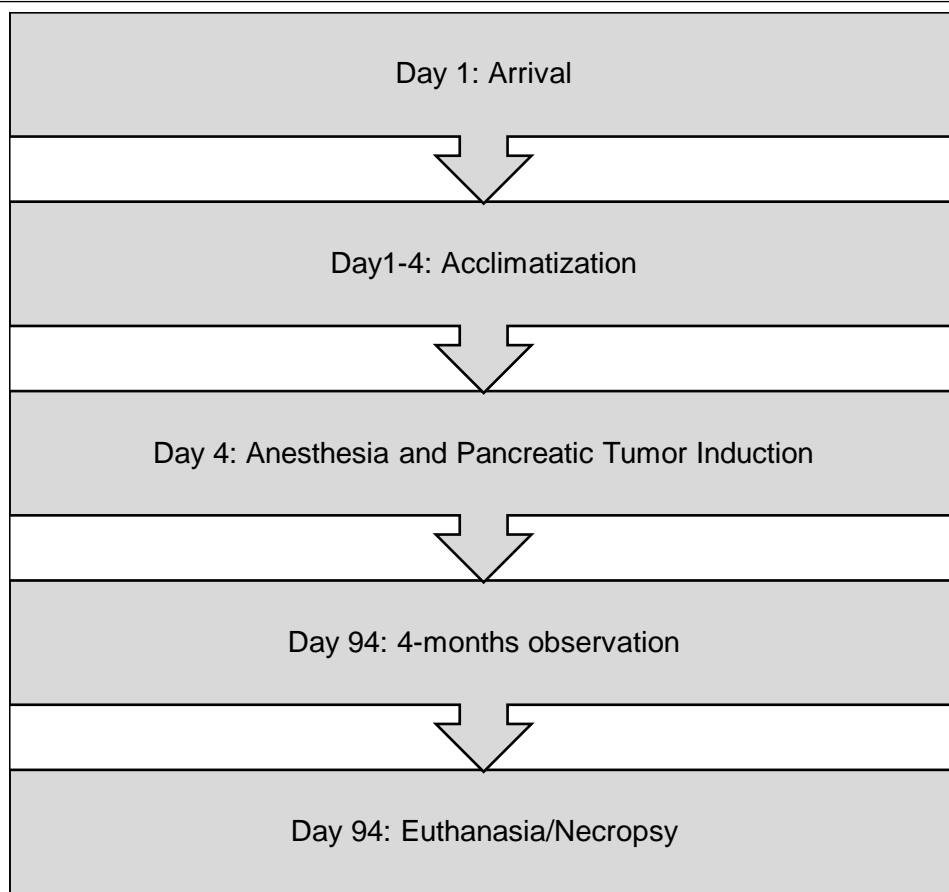


**Figure 23.** Workflow of the Pancreatic Cancer Induction Swine Model

### Sample Selection

Transgenic minipigs, also known as Oncopig Cancer Model or OCM were purchased from the National Swine Research and Resource Center (NSRRC) at the University of Missouri-Columbia and used in this study. [89] Schook et al. used a Cre-Lox system to express transgenic porcine *KRAS*<sup>G12D</sup> and *TP53*<sup>R167H</sup> genes, as described above. [80, 87]

### Animal Welfare

Recommendation from National Institutes of Health detailed in the Guide for the Care and Use of Laboratory Animals (8th ed.) was used to ethically carry out all of the experimental procedures in this study protocol. [43] The animal protocol for the study was reviewed in detail and approved by the Institutional Animal Care and Use Committee of the VA Medical Center in Omaha, Nebraska. The VA Medical Center research facility is approved by Association for Assessment and Accreditation of Laboratory Animal Care International (AAALAC) and all procedures were performed in the AAALAC approved facilities. [43]

### Animal Preparation

Five transgenic minipigs, also known as Oncopig Cancer Model or OCM were purchased from the National Swine Research and Resource Center (NSRRC) at the University of Missouri Columbia. [80, 86] Animals were housed indoors in individual cages under SPF (specific-pathogen free) conditions. During the 3-4-day acclimatization period, the animals had free access to water and were fed a corn and soybean based meal. [46]

### Induction and Anesthesia

Animals were fasted for at least 12 hours before the surgical procedure. [47] During this time, they had free access to drinking water. [47] Anesthesia induction for each animal was with a single 3 mL intra-muscular premixed cocktail injection containing 150 mg Telazol (Zoetis; 4.4mg/kg), 90 mg ketamine (Zoetis; 2.2mg/kg), and 90 mg xylazine (Zoetis; 2.2 mg/kg). [46] To minimize hypersalivation intramuscular atropine sulfate at a dose of 0.05 mg/kg was used on an as needed basis. Each animal was weighed and orotracheally intubated using a 7.0mm - 7.5 mm cuffed tube. [46] A peripheral line was placed in an auricular marginal vein as an additional access to administer fluids or medication. [34, 48, 49] Electrocardiogram monitor, buccal pulse oximeter and rectal temperature probe were placed. To maintain the body temperature at 37 C, animals were rested on a water-circulated heating pad. [34, 48, 49] Anesthesia was maintained with isoflurane (1%-2%) mixed with oxygen (1L-2L). [48] Throughout the procedure animals were mechanical ventilated in a pressure control mode delivering 13-15 breaths/minute, with a tidal volume of 5-10mL/kg, and the end-tidal partial pressure of CO<sub>2</sub> at 30–45 mm Hg. [34, 48, 49]

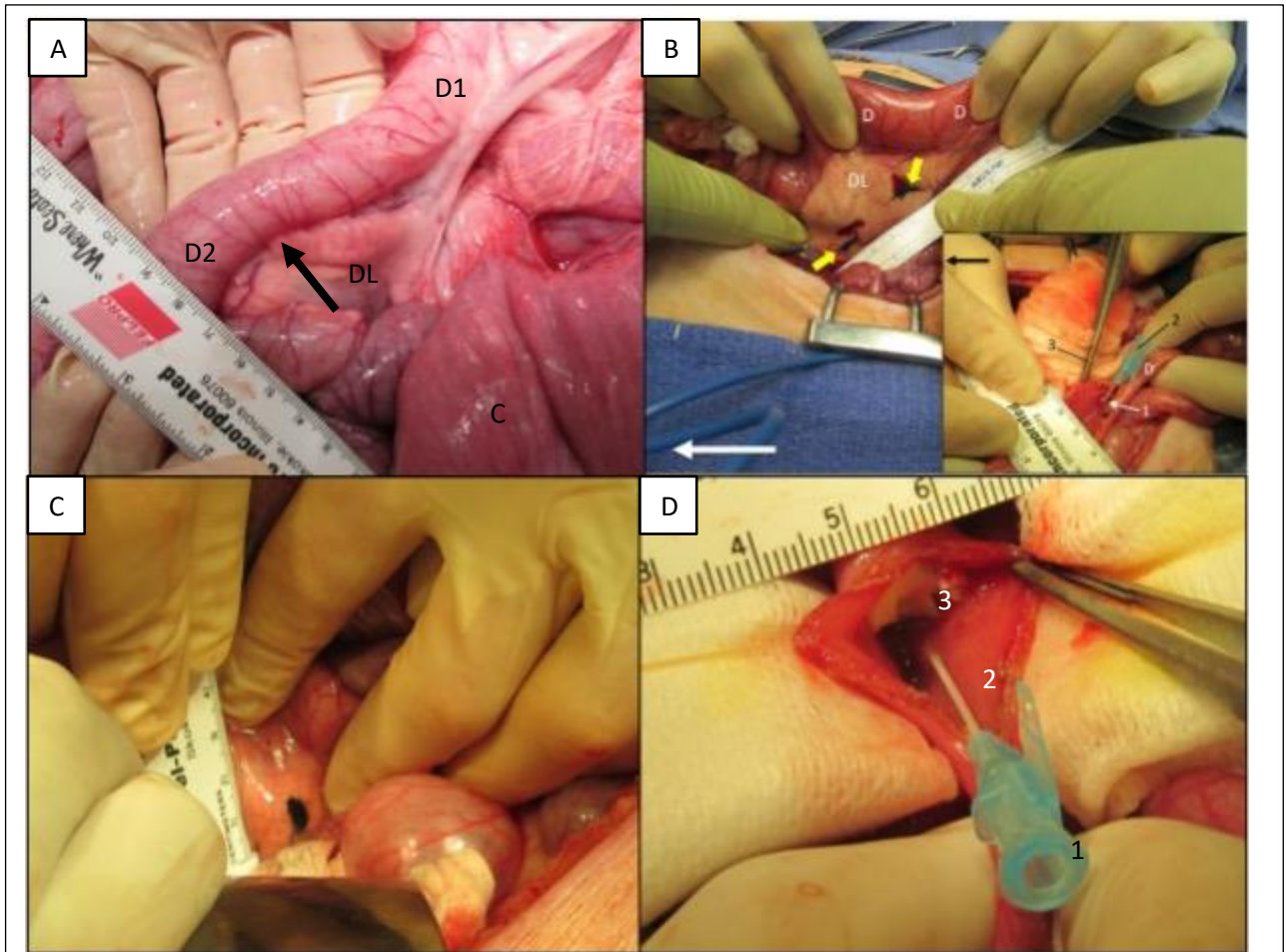
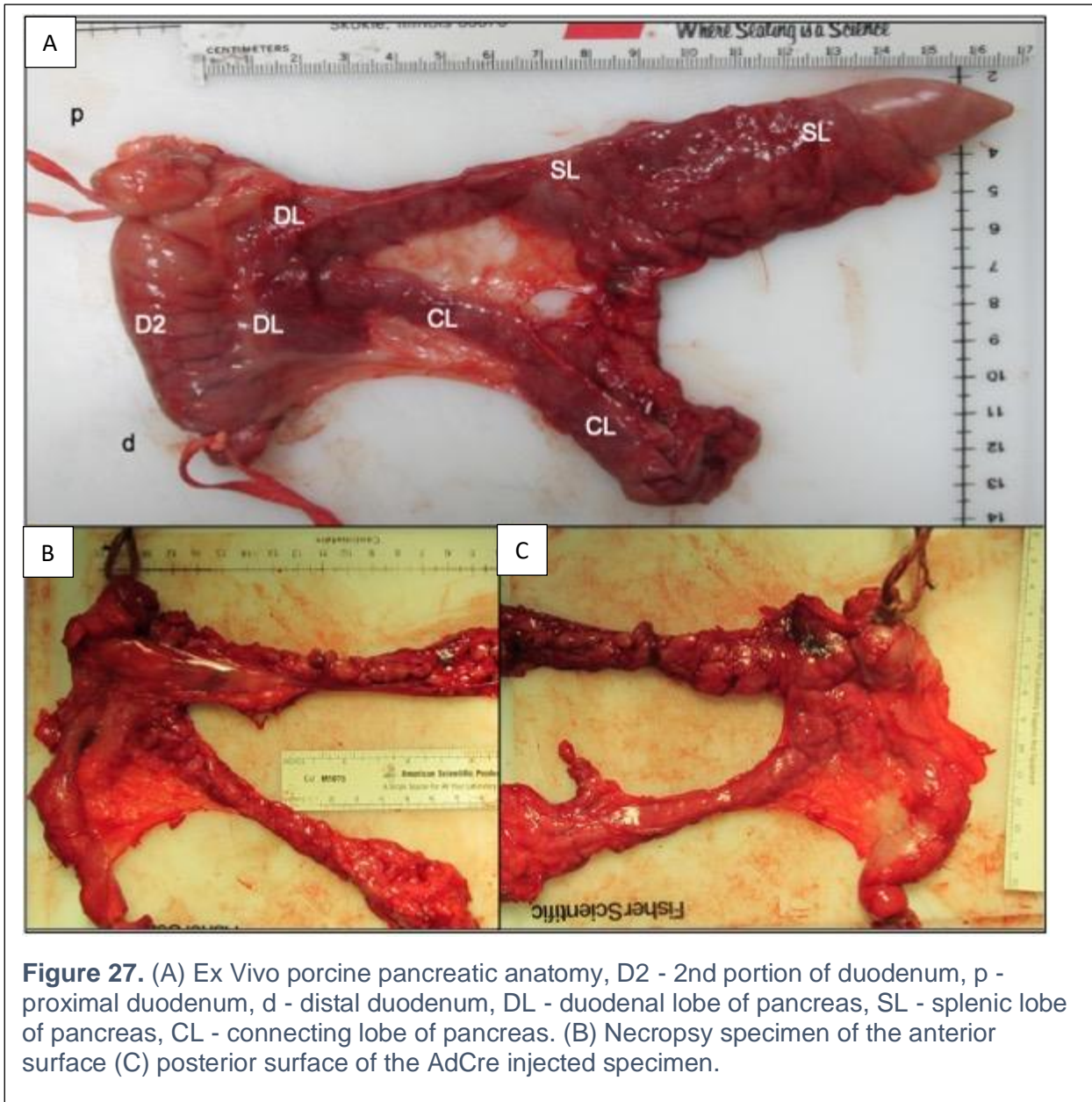


**Figure 25** (A) In vivo porcine pancreatic anatomy. D1 - 1<sup>st</sup> portion of duodenum; D2 - 2<sup>nd</sup> portion of duodenum; DL - duodenal lobe of pancreas; C - colon; Arrow indicates the site where the main pancreatic duct inserts into the duodenum (AdCre injection, site no. 1 (duodenal lobe)). (B) Injection sites for AdCre, yellow arrow – injection site 1, white arrow in inset shows the injection site 2 (C) India ink indicates Cre injection site no. 1, on the posterior surface of the duodenal lobe of the pancreas. (D) India ink indicates Cre injection site no. 2, (1) a 22 g angiocath inserted into (2) main pancreatic duct (3) in the lumen of the duodenum.

### Laparotomy and Tumor Induction

Under aseptic precautions, the animal's abdomen and groin were sterilely prepped and draped. A ventral paramedian laparotomy incision was performed extending from the sternum to the lower abdomen. The incision was then carried to the subcutaneous tissue, musculoaponeurotic layers and peritoneum using a bipolar cautery. A self-retaining abdominal (Bookwalter) retractor was applied along the two sides of the incision. The spleen was retracted, and the pylorus of the stomach was identified, and was used to trace the duodenum and the pancreas. At times the transverse colon had to be retracted inferiorly for adequate exposure of the pancreas.

Next, AdCre (adenovirus expressing Cre recombinase,  $4 \times 10^8$  viral particles in 100  $\mu$ L per site) was injected into the main pancreatic duct, and the pancreatic parenchyma. After identifying the pancreas, a 3-cm longitudinal enterotomy was made along the anti-mesenteric side of the duodenum, following which the main pancreatic duct opening into the duodenum was identified. Using a 22- gauge angiocatheter, AdCre recombinase ( $4 \times 10^8$  viral particles in 100  $\mu$ L) was injected into the main pancreatic duct. Following this, pancreatic parenchyma at two positions were injected with AdCre recombinase ( $4 \times 10^8$  viral particles in 100  $\mu$ L per site) which were marked with india ink. The duodenal enterotomy then was closed in two layers. The abdomen was then closed in three layers and the skin closed with a 4-0 Vicryl suture. The animal was monitored for approximately 4-6 hours in the recovery room and then transferred to their pens.



### Euthanasia and Necropsy

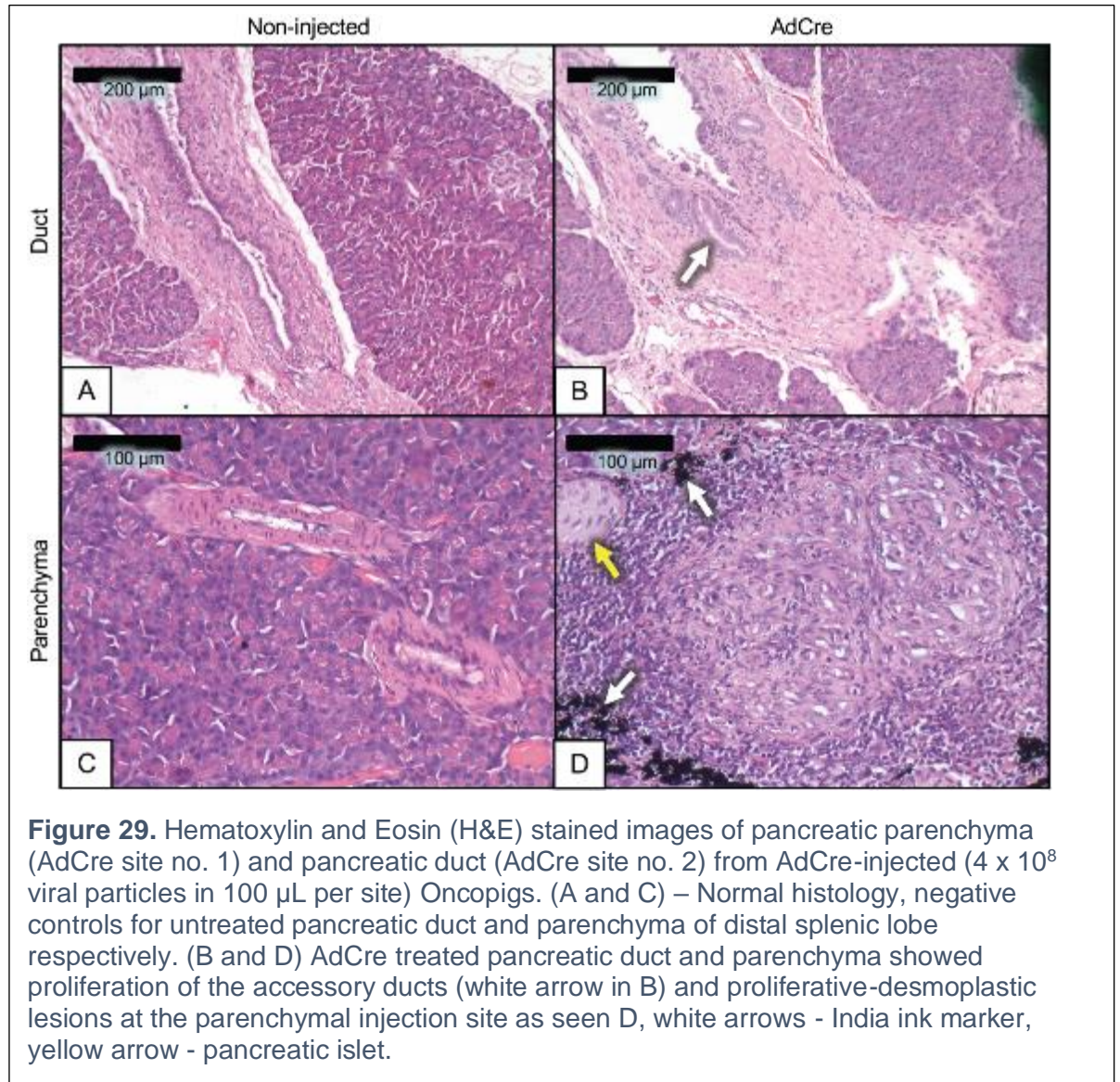
At the end of 3-month observation period after the tumor induction procedure, animals were sedated and orotracheally intubated using standard procedures. [51] The isoflurane inhalation was then increased to 5%. [51] The previous laparotomy incision was opened. [51] The diaphragm was then transversely cut open attempting to expose the supradiaphragmatic inferior vena cava which is then transected. [51] According to AVMA guidelines, death was defined as MAP <10 mm Hg with no identifiable pressure wave tracing. [51] Necropsy specimen of the entire pancreas was obtained and was sent to tissue processing. All suspicious tissues were fixed in formalin and samples stained with H&E for pathological examination.

### Statistical Analysis

Multiple comparisons between the groups were performed by paired t-test (for paired groups of data over time) or ANOVA (for unpaired groups of data at a single time point). All statistical analyses were performed with GraphPad Prism 7.0 software. Data are presented as mean  $\pm$  standard deviation. *P* values of <0.05 will be considered significant.



### 4.3 Results



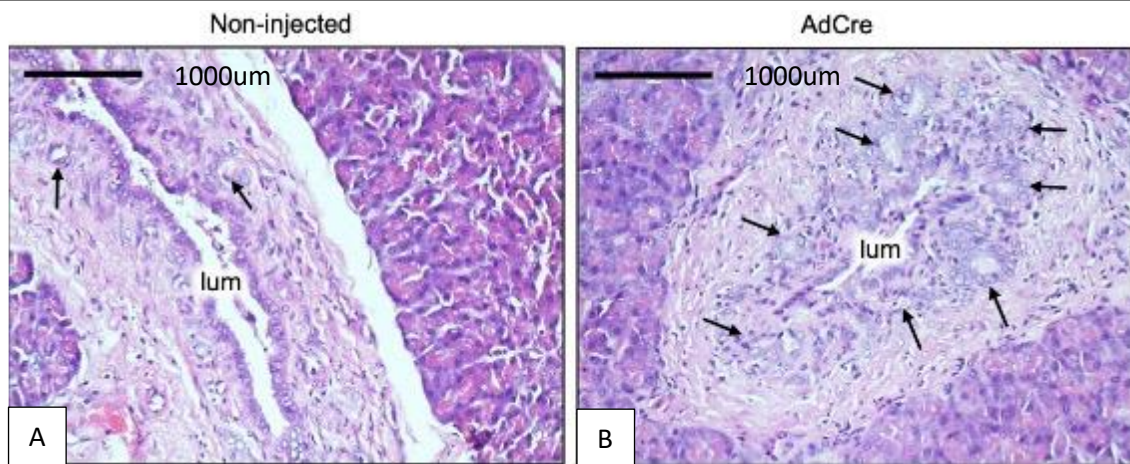


**Figure 31.** Hematoxylin and Eosin (H&E) stained images of the normal (A) and AdCre ( $4 \times 10^8$  viral particles in 100  $\mu$ L per site) injected pancreatic tissue (B). (A) Normal histology, negative control showing untreated pancreatic duct from distal splenic lobe of the pancreas with no accessory ducts. (B) AdCre treated pancreatic duct showing proliferation of the accessory ducts (arrows in B)

lum = lumen of main pancreatic duct.

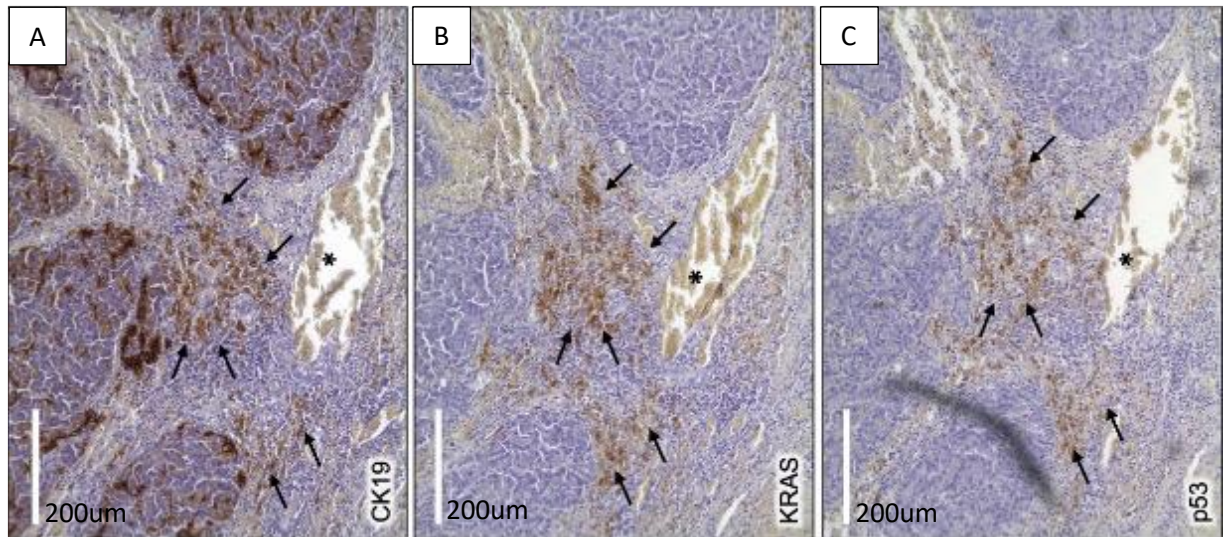


**Figure 33.** Immunohistochemistry (IHC) analysis of paraffin embedded AdCre treated porcine pancreatic tissue. (A) IHC images for CK19 showing nuclear and cytoplasmic staining (btw arrows) of pancreatic duct and pancreatic parenchymal cells. (B) IHC images for KRAS showing nuclear and cytoplasmic staining (btw arrows) of pancreatic duct and pancreatic parenchymal cells. (C) IHC images for p53 showing nuclear and cytoplasmic staining (btw arrows) of pancreatic duct and pancreatic parenchymal cells. (\*) shows an adjacent pancreatic duct

After laparotomy with AdCre injections, all five subjects recovered uneventfully with no peri-operative complications. They were tolerating regular feeds within 3-4 days. Subjects were fed ad lib with regular corn-based meal for 4 mo. Average weight gain during the three-month observation period was around  $30.9 \pm 8.4$  kg for all subjects. Subjects underwent euthanasia with full necropsy at 3 months post-injection of AdCre (subject age 9-10 months). At necropsy, all subjects had intra-abdominal adhesions involving the operative site. Orthotopic implantation of the AdCre recombinase at  $4 \times 10^8$  viral particles in 100  $\mu$ L per site dosage into the main pancreatic duct and pancreatic parenchyma of the Onco-pig did not produce any tangible pancreatic tumor either locally or distally.

Explanted pancreatic tissue from all five animal subjects was fixed in formalin and sent to pathologic analysis. The specimen then underwent serial slicing mainly at the two AdCre injection sites. Tissue was then processed in paraffin and suspicious slices underwent Hematoxylin & Eosin (H&E) staining. Pancreatic tissue from the distal splenic lobe from the same Onco-pig served as a negative control as it was devoid of AdCre injection. Injection site H&E staining did show numerous microscopic proliferative lesions with desmoplastic features (see fig 15 B, D and fig 16 B). Main pancreatic duct epithelium appeared normal except for increased proliferation of accessory ducts around the main pancreatic duct lumen (see fig 15 B and fig 16 B). In contrast, the pancreatic duct from the non-injected region had relatively few accessory ducts around the main duct (see fig 15 A and fig 16 A).

Paraffin blocks which had revealed proliferative-desmoplastic lesions within the Onco-pig pancreatic specimens were re-sectioned; consecutive sections then underwent immunohistochemistry (IHC) (see fig 17 A, B, C). DAB (3,3'-Diaminobenzidine) was used as the primary stain and hematoxylin as the counterstain. IHC images for three genes



*CK19*, *KRAS*, *p53* showed positive nuclear and cytoplasmic staining of pancreatic duct and pancreatic parenchymal cells in and around the injection site. (Fig 17 A, B, C) Interspersed were normal appearing pancreatic parenchyma. (Fig 17 A, B, C)

#### *4.4 Discussion*

More than 95% of the animal models used in Pancreatic cancer research are based on the mouse. [79, 86] While these are excellent tools to study basic molecular biology of cancer, they do not always mirror the heterogeneity and complex tumor characteristics of human cancers. [2, 3, 15, 19] As translational models, murine models show less-than-optimal predictability and validity. [2, 3, 19] Due to their larger size, pigs were expected to produce a tangible resultant pancreatic tumor that can be used study imaging, radiation therapy and photodynamic therapy. [11] Thirdly, tumorigenesis of porcine cells, is similar to human cancer and requires several genetic alterations and will make a highly predictive preclinical model to study anti-cancer therapies. [90] Finally, after standardizing the protocols, production of genetically engineered porcine PC model will be simple, rapid, easy and relevant to human PC.

The histopathological findings in the five Oncopig animals unfortunately did not produce any tumorous growth in the pancreas, however they did show histologic evidence of transgene expression, tissue desmoplasia, and ductal proliferation, suggesting some degree of transformation may have occurred. The lack of gross tumor generation may have been secondary to technical errors- namely, inadequate dosage of the induction cells, inadequate gene alterations etc. For this reason, future projects may involve additional genetic hits for pancreatic cancer or inoculation of larger doses of the transformation inducer (AdCre).

Off note, induction of pancreatic cancer in a large animal model was continued by other members of the Carlson laboratory. In the second set of pancreatic induction cancer model, 16 Oncopig subjects were used and 14 received pancreatic AdCre injection with and without interleukin 8 (IL-8). [89] AdCre recombinase enzyme was injected at a higher dose  $2 \times 10^{10}$ , 100-fold higher than the dose used in the first set of experiments. [89] IL-8, a neutrophil chemotactic factor was used alongside AdCre recombinase to mobilize the receptor to the luminal side of the ductal epithelial cells, which would aid the entry of the virus into the ductal epithelial cells and or exocrine cells. [89] Additionally, some of the subjects underwent ligation and injection of AdCre into the connecting lobe pancreatic duct and connecting lobe pancreatic parenchyma. [89] Nine out of the fourteen Oncopigs developed pancreatic tumor. [89] All of the subjects did not survive the intended length of observation period and expired prematurely within 2-4 weeks of AdCre injection. [89] Subjects developed failure to thrive, florid pancreatitis and pancreatic tumor formation. [89] Authors attributed the intense inflammatory reaction in the pancreas to IL-8 and they would like to design and optimize future studies with appropriate dose of AdCre so that the animals survive the tumor induction without associated severe pancreatitis. [89]

## CHAPTER 5

### *Overall conclusions*

The goal of this research article was to design and characterize three porcine surgical models and effectively use this as a platform to test diagnostic and therapeutic strategies.

- 1) In a non-survival, non-compressible hepatic resection swine model, we previously designed and standardized a grade V liver injury protocol and successfully used this model to evaluate the acute efficacy of a hemostatic patch. This model mimicked truncal non-compressible hemorrhage in combat trauma. In this model of porcine hepatic resection, we show that the resorbable PCL mesh, either alone or in combination with biologics, appeared to have equivalent hemostatic efficacy as the traditional surgical technique.
- 2) In a porcine model of hindlimb ischemia, our aim was to develop an animal model of end-organ disease for peripheral arterial atherosclerosis, in order to have a platform to develop and optimize regenerative therapies. Here after inducing hind limb ischemia in domestic swine, we successfully used FDA approved medical grade real-time X-ray fluoroscopy to shoot peripheral angiographies. We successfully induced ischemia and show measurable difference in end points - arterial pressure, muscle oxygen saturation, and

treadmill stamina between two ligation techniques. Lastly, we developed a tool to test out future regenerative strategies.

- 3) In a novel porcine model of pancreatic cancer, our intention was to induce pancreatic ductal adenocarcinoma in a large animal (transgenic minipig) whose size was comparable with humans, which would provide us with a platform to use and test diagnostic and therapeutic strategies. Here we show that the AdCre injection of the transformed cells into the pancreatic duct and the parenchyma of five Oncopigs after three months failed to produce gross tumors but did show histological evidence cell proliferation with transgene expression.

In conclusion, we show that these porcine surgical models are new attractive intermediate animal models that mirror human disease and stay relevant in the world of translational research. In these models we use advanced medical imaging to better characterize and quantify the disease process which may not be possible in murine animal models. Additionally, we show that these models provide us with unique opportunity to test and develop newer diagnostic methods and therapies.



## CHAPTER 6

### *Future Directions*

- 1) In the non-compressible hepatic resection swine model, although our approach represents a reliable model for examining the efficacy of hemostatic dressings, there are some limitations of this study that should be addressed in future research. Firstly, the battlefield and accident associated traumatic injuries are far more complex in real life than that has been demonstrated in this study. Secondly, the efficacy of the bandages could be affected by wound conditions and the mode of application of biologics. Lastly, the sample size of the study between groups maybe small and additional testing on a larger sample size may produce a different result. The next step in these studies will involve long-term toxicity trials in a larger sample of domestic swine.
- 2) In the porcine model of hindlimb ischemia, ligation and excision of the ilio-femoral complex in domestic swine produced measurable difference in arterial pressure, muscle oxygen saturation, and treadmill stamina, along with histological evidence consistent with myopathy. Further validation of this model is needed to demonstrate the reproducibility and correlation to human pathology. Use of Xray fluoroscopy in this study produced low-resolution angiographic imaging but addition of computerized tomography guided fluoroscopy for the future studies will provide us with high resolution imagery. After standardizing the hindlimb ischemia model, can be used as a tool to test stem cell regenerative therapies.

- 3) Although the porcine model of pancreatic cancer failed to produce gross tumors but did show histological evidence of cell proliferation with transgene expression locally at the site of transformed cell induction. Future studies may involve using additional hits in the genes causing pancreatic cancer. Future studies may also involve injection of the transformed cells into immunocompetent pigs.

## REFERENCES

1. Bryda, E.C., *The Mighty Mouse: the impact of rodents on advances in biomedical research*. Mo Med, 2013. **110**(3): p. 207-11.
2. Mak, I.W., N. Evaniew, and M. Ghert, *Lost in translation: animal models and clinical trials in cancer treatment*. Am J Transl Res, 2014. **6**(2): p. 114-8.
3. Cook, N., D.I. Jodrell, and D.A. Tuveson, *Predictive in vivo animal models and translation to clinical trials*. Drug Discov Today, 2012. **17**(5-6): p. 253-60.
4. Begley, C.G. and L.M. Ellis, *Drug development: Raise standards for preclinical cancer research*. Nature, 2012. **483**(7391): p. 531-3.
5. Swindle, M.M., et al., *Swine as models in biomedical research and toxicology testing*. Vet Pathol, 2012. **49**(2): p. 344-56.
6. Dawson, H. *A Comparative Assessment of the Pig, Mouse and Human Genomes: Structural and Functional Analysis of Genes Involved in Immunity and Inflammation*. 2011.
7. Meurens, F., et al., *The pig: a model for human infectious diseases*. Trends Microbiol, 2012. **20**(1): p. 50-7.
8. Swearengen, J.R., *Choosing the right animal model for infectious disease research*. Animal Model Exp Med, 2018. **1**(2): p. 100-108.
9. Kararli, T.T., *Comparison of the gastrointestinal anatomy, physiology, and biochemistry of humans and commonly used laboratory animals*. Biopharm Drug Dispos, 1995. **16**(5): p. 351-80.
10. Perleberg, C., A. Kind, and A. Schnieke, *Genetically engineered pigs as models for human disease*. Dis Model Mech, 2018. **11**(1).

11. Sieren, J.C., et al., *Development and translational imaging of a TP53 porcine tumorigenesis model*. J Clin Invest, 2014. **124**(9): p. 4052-66.
12. Ericsson, A.C., M.J. Crim, and C.L. Franklin, *A brief history of animal modeling*. Mo Med, 2013. **110**(3): p. 201-5.
13. Hickman, D.L., et al., *Commonly Used Animal Models*. Principles of Animal Research for Graduate and Undergraduate Students, 2017: p. 117-175.
14. Linder, C.C., *Mouse nomenclature and maintenance of genetically engineered mice*. Comp Med, 2003. **53**(2): p. 119-25.
15. Denayer, T., T. Stöhr, and M. Van Roy, *Animal models in translational medicine: Validation and prediction*. New Horizons in Translational Medicine, 2014. **2**(1): p. 5-11.
16. Waterston, R.H., et al., *Initial sequencing and comparative analysis of the mouse genome*. Nature, 2002. **420**(6915): p. 520-62.
17. Cheon, D.J. and S. Orsulic, *Mouse models of cancer*. Annu Rev Pathol, 2011. **6**: p. 95-119.
18. Bailey, K.L. and M.A. Carlson, *Porcine Models of Pancreatic Cancer*. Front Oncol, 2019. **9**: p. 144.
19. Dawson, H.D., et al., *The porcine translational research database: a manually curated, genomics and proteomics-based research resource*. BMC Genomics, 2017. **18**(1): p. 643.
20. Walters, E.M., et al., *Completion of the swine genome will simplify the production of swine as a large animal biomedical model*. BMC Med Genomics, 2012. **5**: p. 55.
21. Helke, K.L., et al., *Pigs in Toxicology: Breed Differences in Metabolism and Background Findings*. Toxicol Pathol, 2016. **44**(4): p. 575-90.
22. Schomberg, D.T., et al., *Miniature Swine for Preclinical Modeling of Complexities of Human Disease for Translational Scientific Discovery and Accelerated*

- Development of Therapies and Medical Devices*. Toxicol Pathol, 2016. **44**(3): p. 299-314.
23. Murphy, S.L., et al., *Deaths: Final Data for 2018*. Natl Vital Stat Rep, 2021. **69**(13): p. 1-83.
  24. Sauaia, A., et al., *Epidemiology of trauma deaths: a reassessment*. J Trauma, 1995. **38**(2): p. 185-93.
  25. Oyeniyi, B.T., et al., *Trends in 1029 trauma deaths at a level 1 trauma center: Impact of a bleeding control bundle of care*. Injury, 2017. **48**(1): p. 5-12.
  26. Arias, E. and J. Xu, *United States Life Tables, 2018*. Natl Vital Stat Rep, 2020. **69**(12): p. 1-45.
  27. Dutton, R.P., et al., *Trauma mortality in mature trauma systems: are we doing better? An analysis of trauma mortality patterns, 1997-2008*. J Trauma, 2010. **69**(3): p. 620-6.
  28. Toroyan, T., M.M. Peden, and K. Laych, *WHO launches second global status report on road safety*. Inj Prev, 2013. **19**(2): p. 150.
  29. Dellinger, A.M. and D.A. Sleet, *From modest beginnings to a winnable battle: road safety efforts at CDC's Injury Center*. J Safety Res, 2012. **43**(4): p. 279-82.
  30. Baker, S.P., *Injuries: the neglected epidemic: Stone lecture, 1985 America Trauma Society Meeting*. J Trauma, 1987. **27**(4): p. 343-8.
  31. Donley, E.R. and J.W. Loyd, *Hemorrhage Control*, in *StatPearls*. 2021, StatPearls Publishing. Copyright © 2021, StatPearls Publishing LLC.: Treasure Island (FL).
  32. Bennett, B.L., *Bleeding Control Using Hemostatic Dressings: Lessons Learned*. Wilderness Environ Med, 2017. **28**(2s): p. S39-s49.
  33. Kheirabadi, B., *Evaluation of topical hemostatic agents for combat wound treatment*. US Army Med Dep J, 2011: p. 25-37.

34. Holcomb, J.B., et al., *Effect of dry fibrin sealant dressings versus gauze packing on blood loss in grade V liver injuries in resuscitated swine*. J Trauma, 1999. **46**(1): p. 49-57.
35. Calcaterra, J., et al., *Recombinant Human Fibrinogen That Produces Thick Fibrin Fibers with Increased Wound Adhesion and Clot Density*. Biomacromolecules, 2013. **14**(1): p. 169-178.
36. Furie, B. and B.C. Furie, *Mechanisms of thrombus formation*. N Engl J Med, 2008. **359**(9): p. 938-49.
37. Roddie, P.H. and C.A. Ludlam, *Recombinant coagulation factors*. Blood Reviews, 1997. **11**(4): p. 169-177.
38. Pathepchoti Wong, K., P. Tantiniti, and C. Sutthithampanich, *Study of normal values in coagulation profile*. J Med Assoc Thai, 2001. **84**(6): p. 877-81.
39. Sari, I., et al., *Multiple myeloma presenting with acquired factor VIII inhibitor*. Int J Hematol, 2009. **90**(2): p. 166-169.
40. Ofosu, F.A., J. Freedman, and J.W. Semple, *Plasma-derived biological medicines used to promote haemostasis*. Thromb Haemost, 2008. **99**(5): p. 851-62.
41. Carlson, M.A., et al., *A totally recombinant human fibrin sealant*. Journal of Surgical Research, 2014. **187**(1): p. 334-342.
42. Kheirabadi, B.S., et al., *Development of a standard swine hemorrhage model for efficacy assessment of topical hemostatic agents*. J Trauma, 2011. **71**(1 Suppl): p. S139-46.
43. National Research Council Committee for the Update of the Guide for the, C. and A. Use of Laboratory, *The National Academies Collection: Reports funded by National Institutes of Health*, in *Guide for the Care and Use of Laboratory Animals*. 2011, National Academies Press (US). Copyright © 2011, National Academy of Sciences.: Washington (DC).

44. Neter J, W.W., Kutner MH. , *Applied Linear Statistical Models 3rd ed.* Boston. Boston: Irwin Publishing Co, 1990.
45. Chen, S., et al., *New forms of electrospun nanofiber materials for biomedical applications.* J Mater Chem B, 2020. **8**(17): p. 3733-3746.
46. Swindle MM, S.A., *Swine in the Laboratory: Surgery, Anesthesia, Imaging, and Experimental Techniques* 3rd ed. Boca Raton, FL: CRC Press, 2016.
47. Yanala, U.R., et al., *Fluid administration rate for uncontrolled intraabdominal hemorrhage in swine.* PloS one, 2018. **13**(11): p. e0207708-e0207708.
48. Yanala, U.R., et al., *Development of a fatal noncompressible truncal hemorrhage model with combined hepatic and portal venous injury in normothermic normovolemic swine.* PLoS One, 2014. **9**(9): p. e108293.
49. Duggan, M.J., et al., *Development of a lethal, closed-abdomen grade V hepato-portal injury model in non-coagulopathic swine.* J Surg Res, 2013. **182**(1): p. 101-7.
50. Moser, P., *Out of Control? Managing Baseline Variability in Experimental Studies with Control Groups*, in *Good Research Practice in Non-Clinical Pharmacology and Biomedicine*, A. Beshpalov, M.C. Michel, and T. Steckler, Editors. 2020, Springer International Publishing: Cham. p. 101-117.
51. *American Veterinary Medical Association Panel on Euthanasia. AVMA Guidelines for the Euthanasia of Animals: 2013 Edition Schaumburg, IL: American Veterinary Medical Association;. 2013.*
52. Levy, J.H. and L.T. Goodnough, *How I use fibrinogen replacement therapy in acquired bleeding.* Blood, 2015. **125**(9): p. 1387-93.
53. Martini, W.Z., *Fibrinogen availability and coagulation function after hemorrhage and resuscitation in pigs.* Molecular medicine (Cambridge, Mass.), 2011. **17**(7-8): p. 757-761.

54. Lada, E., et al., *Porcine Liver Anatomy Applied to Biomedicine*. J Surg Res, 2020. **250**: p. 70-79.
55. Strandness, D.E., Jr. and J.F. Eidt, *Peripheral vascular disease*. Circulation, 2000. **102**(20 Suppl 4): p. Iv46-51.
56. Shabani Varaki, E., et al., *Peripheral vascular disease assessment in the lower limb: a review of current and emerging non-invasive diagnostic methods*. Biomed Eng Online, 2018. **17**(1): p. 61.
57. Sontheimer, D.L., *Peripheral vascular disease: diagnosis and treatment*. Am Fam Physician, 2006. **73**(11): p. 1971-6.
58. Shu, J. and G. Santulli, *Update on peripheral artery disease: Epidemiology and evidence-based facts*. Atherosclerosis, 2018. **275**: p. 379-381.
59. Conte, M.S., et al., *Global vascular guidelines on the management of chronic limb-threatening ischemia*. J Vasc Surg, 2019. **69**(6s): p. 3S-125S.e40.
60. Kinlay, S., *Management of Critical Limb Ischemia*. Circulation. Cardiovascular interventions, 2016. **9**(2): p. e001946-e001946.
61. Long, C., et al., *A Novel Large-Animal Model of Peripheral Arterial Disease*. Journal of Vascular Surgery, 2016. **63**: p. 293-294.
62. Krishna, S.M., S.M. Omer, and J. Golledge, *Evaluation of the clinical relevance and limitations of current pre-clinical models of peripheral artery disease*. Clin Sci (Lond), 2016. **130**(3): p. 127-50.
63. Simons, M., *Angiogenesis: where do we stand now?* Circulation, 2005. **111**(12): p. 1556-66.
64. Buschmann, I. and W. Schaper, *Arteriogenesis Versus Angiogenesis: Two Mechanisms of Vessel Growth*. News Physiol Sci, 1999. **14**: p. 121-125.
65. Yoder, M.C., et al., *Redefining endothelial progenitor cells via clonal analysis and hematopoietic stem/progenitor cell principals*. Blood, 2007. **109**(5): p. 1801-9.



66. Faber, J.E., et al., *A brief etymology of the collateral circulation*. Arteriosclerosis, thrombosis, and vascular biology, 2014. **34**(9): p. 1854-1859.
67. Feldmann, A., R. Schmitz, and D. Erlacher, *Near-infrared spectroscopy-derived muscle oxygen saturation on a 0% to 100% scale: reliability and validity of the Moxy Monitor*. Journal of Biomedical Optics, 2019. **24**(11): p. 115001.
68. O'Konski, M.S., et al., *Ameroid constriction of the proximal left circumflex coronary artery in swine. A model of limited coronary collateral circulation*. Am J Cardiovasc Pathol, 1987. **1**(1): p. 69-77.
69. Keeran, K.J., et al., *A Chronic Cardiac Ischemia Model in Swine Using an Ameroid Constrictor*. Journal of visualized experiments : JoVE, 2017(128): p. 56190.
70. Wang, T., et al., *Evaluation of skeletal muscle perfusion in canine hind limb ischemia model using color-coded digital subtraction angiography*. Microvascular Research, 2019. **123**: p. 81-85.
71. Waters, R.E., et al., *Preclinical models of human peripheral arterial occlusive disease: implications for investigation of therapeutic agents*. J Appl Physiol (1985), 2004. **97**(2): p. 773-80.
72. Ojalvo, A.G., et al., *Therapeutic angiogenesis following intramuscular gene transfer of vascular endothelial growth factor 121 in a dog model of hindlimb ischemia*. Electronic Journal of Biotechnology, 2003. **6**: p. 208-222.
73. Ilic, M. and I. Ilic, *Epidemiology of pancreatic cancer*. World journal of gastroenterology, 2016. **22**(44): p. 9694-9705.
74. Rawla, P., T. Sunkara, and V. Gaduputi, *Epidemiology of Pancreatic Cancer: Global Trends, Etiology and Risk Factors*. World journal of oncology, 2019. **10**(1): p. 10-27.
75. Society, A.C., *Cancer Facts & Figures 2021*. Atlanta: American Cancer Society; 2021, 2021.

76. Facts, S.C.S., *Pancreatic Cancer*. . National Cancer Institute. Bethesda, MD, 2020.
77. Hidalgo, M., *Pancreatic cancer*. N Engl J Med, 2010. **362**(17): p. 1605-17.
78. Maitra, A. and R.H. Hruban, *Pancreatic cancer*. Annual review of pathology, 2008. **3**: p. 157-188.
79. Herreros-Villanueva, M., et al., *Mouse models of pancreatic cancer*. World journal of gastroenterology, 2012. **18**(12): p. 1286-1294.
80. Schook, L.B., et al., *A Genetic Porcine Model of Cancer*. PLoS One, 2015. **10**(7): p. e0128864.
81. Kalla, D., A. Kind, and A. Schnieke, *Genetically Engineered Pigs to Study Cancer*. Int J Mol Sci, 2020. **21**(2).
82. Boas, F.E., et al., *Induction and characterization of pancreatic cancer in a transgenic pig model*. PLoS One, 2020. **15**(9): p. e0239391.
83. Flisikowska, T., A. Kind, and A. Schnieke, *Pigs as models of human cancers*. Theriogenology, 2016. **86**(1): p. 433-7.
84. Robertson, N., L.B. Schook, and K.M. Schachtschneider, *Porcine cancer models: potential tools to enhance cancer drug trials*. Expert Opin Drug Discov, 2020. **15**(8): p. 893-902.
85. Xu, C., et al., *Translating Human Cancer Sequences Into Personalized Porcine Cancer Models*. Front Oncol, 2019. **9**: p. 105.
86. Schachtschneider, K.M., et al., *The Oncopig Cancer Model: An Innovative Large Animal Translational Oncology Platform*. Frontiers in oncology, 2017. **7**: p. 190-190.
87. Schachtschneider, K.M., et al., *Oncopig Soft-Tissue Sarcomas Recapitulate Key Transcriptional Features of Human Sarcomas*. Sci Rep, 2017. **7**(1): p. 2624.
88. Schachtschneider, K.M., et al., *A validated, transitional and translational porcine model of hepatocellular carcinoma*. Oncotarget, 2017. **8**(38): p. 63620-63634.

89. Patel, N.S., et al., *Induction of pancreatic neoplasia in the <em>KRAS/TP53</em> Oncopig: preliminary report*. bioRxiv, 2020: p. 2020.05.29.123547.
90. Adam, S.J., et al., *Genetic induction of tumorigenesis in Swine*. Oncogene, 2007. **26**(7): p. 1038-1045.